Calibration of Non-Lane Based Macroscopic Continuum Model-Using Global Search Algorithms

Hari Krishna Gaddam, **K. Ramachandra Rao**

Department of Civil Engineering and
Transportation Research and Injury Prevention Programmme (TRIPP)
Indian Institute of Technology Delhi, India

Outline

- Model development
- Calibration methodology
- Results and sensitivity analysis

Heterogeneous traffic stream with non-lane discipline

- Different operational and performance characteristics
- High degree of variation in physical and dynamical characteristics of vehicles
- Motorised two wheelers have high degree of manoeuvrability
- Use same right of way – no lane discipline
- Continuous longitudinal and lateral movement of vehicles

Background- lane based models

- PW–type models (Payne 1971, Payne 1979, Kühne & Rödiger 1991, Michalopoulos et al. 1993, Berg et al. 2000, Gupta & Katiyar 2006) produce some non-physical solutions such as isotropy, wrong way travel and fluid like behavior
- Anisotropic models (Aw & Rascle 2000, Zhang 2002, Jiang et al. 2002, Huang et al. 2006, Tang et al. 2007, Gupta and Katiyar, 2007, Tang et al. 2009, Chuan et al. 2012, Cheng et al. 2017, Cheng et al. 2017) are developed to overcome the deficiencies present in PW-type models
- The key assumption behind these theories is that the vehicles strictly travel at the centre of the lane and they assign leadership fully to the front vehicle
- The models mentioned above are only restricted to lane based traffic environment and can not be applied directly to non-lane environment

Background- Non-lane based models

- Nair et al. (2011) porous flow model based on static speed – pore size density relationship. Difficult to apply more than two vehicle classes
- Gupta and Dhiman (2014) - one-sided lateral gap continuum model. It can only describe the vehicle movement on a single lane road. It does not take in to account the interaction between slow moving and fast moving vehicle and no viscosity
- Mohan and Ramadurai (2017) extended Aw-Rascale model using area occupancy. Vehicle momentum conserved separately; vehicles off-centeredness and the interaction between slow moving vehicles and fast moving vehicles are not considered

Non-lane based car following model

Non-lane based FVD car following model with Two Side Lateral Gaps (Li et al., 2015)

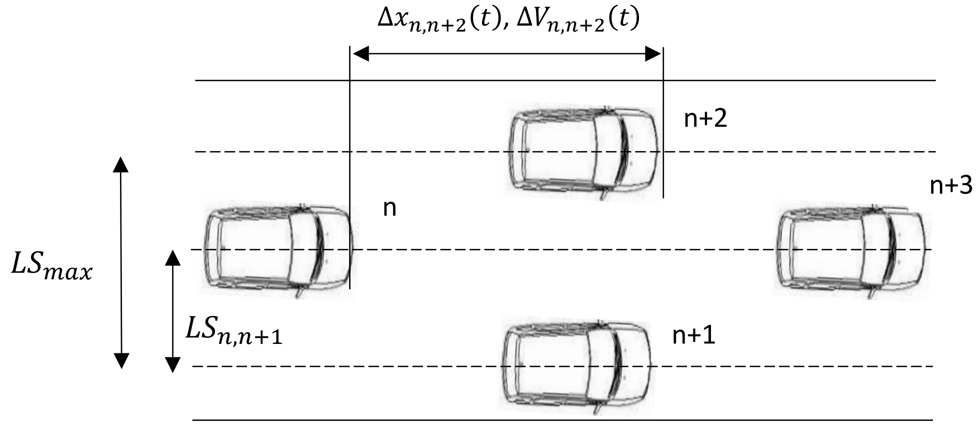

Fig 1: Lane separation Behaviour

Case 1:

$LS_{n,n+1} \in [0, 0.5\, LS_{max}]$

$$a_n(t) = \alpha\{V[(1-2p_n)\Delta x_{n,n+1}(t) + 2p_n \Delta x_{n,n+3}(t)] - V_n(t)\} + k[(1-2p_n)\Delta V_{n,n+1}(t) + 2p_n \Delta V_{n,n+3}(t)$$

Case 2:

$LS_{n,n+1} \in [0.5\, LS_{max}, LS_{max}]$

$$a_n(t) = \alpha\{V[(2p_n-1)\Delta x_{n,n+2}(t) + 2(1-p_n)\Delta x_{n,n+3}(t)] - V_n(t)\} + k[(2p_n-1)\Delta V_{n,n+2}(t) + 2(1-p_n)\Delta V_{n,n+3}(t$$

Here $p_n = \frac{LS_{n,n+1}}{LS_{max}}$, LS_{max} Can be chosen as 3.5 m. Consistent with typical road width

Modified non-lane based heterogeneous car following model

The acceleration of vehicle class i with respect to any one condition such as $LS_{n,n+1} \in [0, 0.5\, LS_{max}]$ is equivalent to:

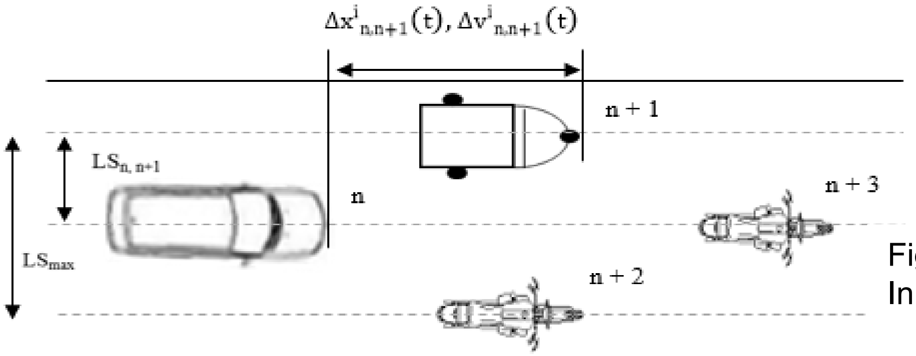

Fig 2: Lane separation Behavior
In heterogeneous traffic stream

$$a^i_n(t) = \alpha_i \left\{ V\left[(1 - 2p_n)\Delta x^i_{n,n+1}(t) + 2p_n \Delta x^i_{n,n+3}(t) \right] - V^i_n(t) \right\} + \kappa_i \left[(1 - 2p_n)\Delta v^i_{n,n+1}(t) + 2p_n \Delta v^i_{n,n+3}(t) \right]$$

here: $\Delta x^i_{n,n+1}(t) = \sum_{j=1}^{N} P_{ij} \left(x^j_{n+1}(t) - x^i_n(t) \right)$, $\Delta v^i_{n,n+1}(t) = \sum_{j=1}^{N} P_{ij} \left(v^j_{n+1}(t) - v^i_n(t) \right)$ are space headway and speed of vehicle class i respectively. N is the number of vehicle classes. P_{ij} is the number of times vehicle class i followed vehicle class j. T_i and τ_i are the reactive coefficient of vehicle class i.

Micro-Macro connection

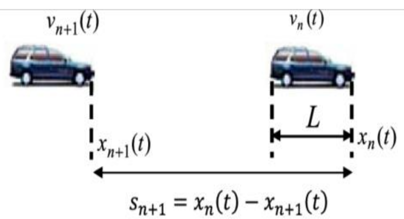

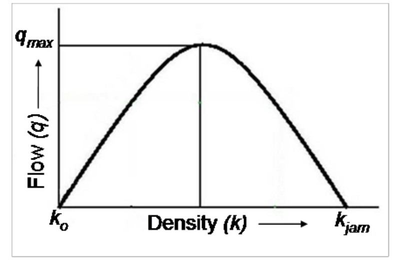

Variable	Micro	Macro
Spatial Headway → Density	$\Delta x = x_n(t) - x_{n+1}(t)$	k
Optimum velocity → Equilibrium velocity	$\mathrm{V}\left[(1-2\mathrm{p_n})\Delta \mathrm{x^i}_{\mathrm{n,n+1}}(\mathrm{t}) + 2\mathrm{p_n}\Delta \mathrm{x^i}_{\mathrm{n,n+3}}(\mathrm{t})\right]$	$\mathrm{V_{ie}}\left(\frac{\mathrm{k(x,t)}}{1+2*\delta_\mathrm{i}}\right)$
Individual speeds	$\mathrm{V^i}_\mathrm{n}(\mathrm{t})$, $\mathrm{V^j}_{\mathrm{n+1}}(\mathrm{t})$, $\mathrm{V^j}_{\mathrm{n+2}}(\mathrm{t})$, $\mathrm{V^j}_{\mathrm{n+3}}(\mathrm{t})$	$\mathrm{V_i(x,t)}, \mathrm{V_j(x+\Delta x,t)}, \mathrm{V_j(x+\Delta x,t)}, \mathrm{V_j(x+2\Delta x,t)}$
Reactive coefficients	α_i, k_i, P_{ij}	$\frac{1}{\tau_{ij}}, \frac{1}{T_i}, P_j(\mathrm{x}+\Delta_j, \mathrm{t})$
Example: FVD → SG model	$\frac{d\mathrm{v}_{\mathrm{n+1}}(\mathrm{t})}{dt} = k[\mathrm{v}(\Delta \mathrm{x}) - \mathrm{v}_{\mathrm{n+1}}(\mathrm{t})] + \lambda\Delta \mathrm{v}$	$\frac{\partial \mathrm{v}}{\partial \mathrm{t}} + \mathrm{v}\frac{\partial \mathrm{v}}{\partial \mathrm{x}} = \frac{\mathrm{v_e} - \mathrm{v}}{\tau} - c_0\frac{\partial \mathrm{v}}{\partial \mathrm{x}}$

Non-lane based heterogeneous continuum model

After applying variable transformation and Taylor series expansion, we obtain:

$$\frac{\partial k_i}{\partial t} + \frac{\partial k_i v_i}{\partial x} = 0 \qquad (ia)$$

$$\frac{\partial V_i}{\partial t} + V_i \frac{\partial V_i}{\partial x} = \frac{1}{T_i}\left[V_{ie}\left({}^{k}\!/_{1 + 2\delta_i}\right) - V_i\right] + \frac{1}{\tau_i}(1 + 2\delta_i)\sum_{j=1}^{N} P_j \Delta x \frac{\partial V_j}{\partial x}$$

$$+ \frac{1}{\tau_i}\left(\frac{1 + 6\delta_i}{2}\right)\sum_{j=1}^{N} P_j\, \Delta x^2 \frac{\partial^2 V_j}{\partial x^2}$$

$$+ \frac{1}{\tau_i}\sum_{j=1}^{N} P_j\left(\mathrm{V_j(x,t)} - \mathrm{V_i(x,t)}\right) \qquad (iia)$$

Effect of lateral separation distance on longitudinal headway

Lateral separation distance values for various vehicle combinations

Follower-leader vehicle types	LSD factor for each vehicle combinations (δ_{ij})	LSD factor for each vehicle class (δ_i)
Car-Car	0.24	0.25
Car-MTW	0.22	
Car-MThW	0.33	
Car-HV	0.57	
MTW-Car	0.28	0.24
MTW-MTW	0.18	
MTW-MThW	0.30	
MTW-HV	0.51	
MThW-Car	0.35	0.29
MThW-MTW	0.19	
MThW-MThW	0.33	
MThW -HV	0.74	
HV-All	0.26	0.26

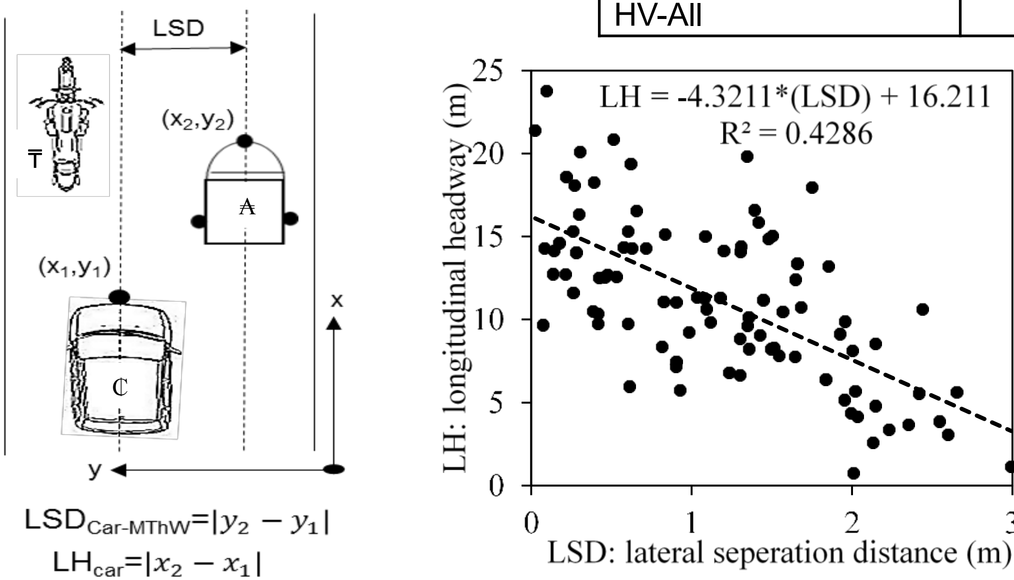

(a)

(b)

Figure 3: Relationship between longitudinal headway and lateral separation distance of Car and MThW (a) Schematic representation (b) Regression plot (Here x = longitudinal co-ordinate, y=lateral co-ordinate, ₸= MTW, ₳=MThW, ₵= Car)

Effect of frictional clearance between vehicles

Frictional clearance regression statistics

Response variable	Predictor variables	Coefficients	t-statistics	p-value	R^2-value
Car speed	Intercept	11.81	16.18	0.00	0.63
	frictional clearance	4.40	6.14	0.00	
MTW speed	Intercept	15.68	12.86	0.00	0.04
	frictional clearance	1.57	1.19	0.24	
MThW speed	Intercept	14.24	8.80	0.00	0.05
	frictional clearance	1.78	1.31	0.21	
HV speed	Intercept	13.45	5.60	0.00	0.04
	frictional clearance	1.28	0.74	0.47	

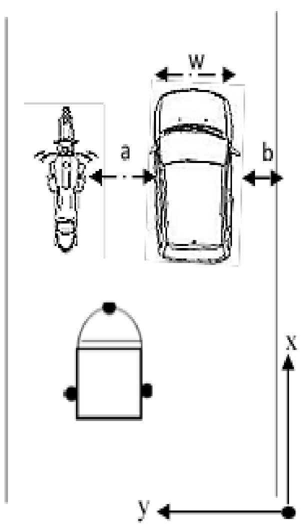

(a)

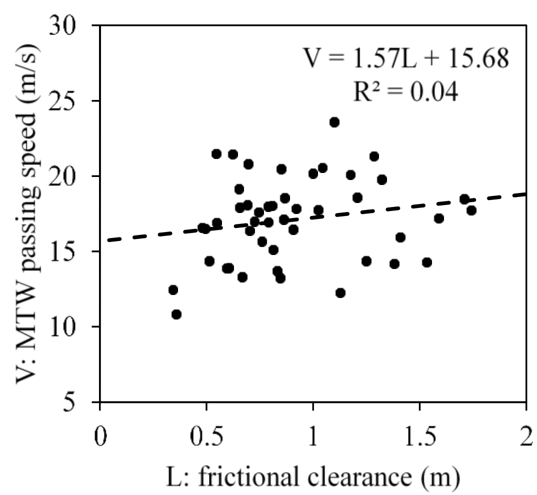

(b)

Figure 4: Relationship between frictional clearance and passing speed of car and MTW (a) Schematic representation (b) Regression plot (Here x=longitudinal co-ordinate, y=lateral co-ordinate and $a = |y_2 - y_1| - \left(\frac{w_1+w_2}{2}\right)$, a = frictional clearance between car and MTW, w_1 = width of a MTW, w_2 = width of a Car, b = frictional clearance between car and median)

Non-lane based heterogeneous traffic (NLHT) continuum model with driver memory and sideways friction

$$\frac{\partial k_i}{\partial t} + \frac{\partial k_i v_i}{\partial x} = 0 \qquad (ib)$$

$$\frac{\partial V_i}{\partial t} + V_i \frac{\partial V_i}{\partial x} - (1 + 2\delta_i) \sum_{j=1}^{N} P_j \mathrm{c_j}(k) \frac{\partial V_j}{\partial x} \qquad (iib)$$

$$= \frac{1}{T_i}\left[V_{ie}\left({}^{k}/_{1 + 2\delta_i}\right) - V_i\right] + \left(\frac{1 + 6\delta_i}{2}\right) \sum_{j=1}^{N} P_j\, c^2{}_j(k) \tau_i \frac{\partial^2 V_j}{\partial x^2}$$

$$+ \sum_{j\ (\neq i)}^{N} \mu_{ij} \frac{P_j}{\tau_i} (\mathrm{V_j} - \mathrm{V_i})$$

- Here: $\delta_i = \sum_{j=1}^{N} p_{ij}\delta_{ij}$ and $\delta_{ij} = \frac{LSD_{ij}}{3.5}$ is a lateral separation distance parameter, T_i and τ_i are driver reactive coefficients
- Disturbance propagation speed

$$\mathrm{c_j}(k) = -k * V'_{je}(k), \left(\frac{\Delta \mathrm{x}}{\tau_\mathrm{i}}\right)^2 * \tau_\mathrm{i} = \mathrm{c^2{}_j(k)} * \tau_\mathrm{i} = \left(-\mathrm{k} * \mathrm{V'_{je}(k)}\right)^2 * \tau_\mathrm{i}, \tau_{ij} = \tau_j$$

- Further, frictional clearance factor $\mu_{ij} = 1\ if\ V_{if} > V_{jf}$ otherwise zero

Equilibrium function

- Equilibrium Equation fitted from empirical data:

$$\mathrm{v}_{ie} = \frac{\mathrm{v}_{\mathrm{if}}\left[1 - \left(\frac{k_i}{\mathrm{k}_{\mathrm{jam}}}\right)^{\mathrm{a}}\right]^{\mathrm{b}}}{1 + \mathrm{E}\left(\frac{k_i}{\mathrm{k}_{jam}}\right)^{\theta}} \qquad (iii)$$

Here, V_{if}, k_{jam} are traffic stream parameters; a, b, E and θ are shape parameters

Vector form of the model

$$U_t + f(U)_x = S(U)$$

Where

$$U = \begin{pmatrix} K_1 \\ V_1 \\ K_2 \\ V_2 \\ . \\ . \\ K_N \\ V_N \end{pmatrix} \qquad \mathrm{f}(U) = \begin{bmatrix} K_1 V_1 \\ \frac{V_1^2}{2} - (1 + 2\delta_1) \sum_{j=1}^{N} P_j \mathrm{c_j}(k) V_j \\ K_2 V_2 \\ \frac{V_2^2}{2} - (1 + 2\delta_2) \sum_{j=1}^{N} P_j \mathrm{c_j}(k) V_j \\ . \\ . \\ . \\ K_N V_N \\ \frac{V_N^2}{2} - (1 + 2\delta_N) \sum_{j=1}^{N} P_j \mathrm{c_j}(k) V_j \end{bmatrix}$$

$$S(U) = \begin{bmatrix} 0 \\ \frac{1}{T_1}\left[V_{1e}\left({k}/{1+2\delta_1}\right) - V_1\right] + \left(\frac{1+6\delta_1}{2}\right)\sum_{j=1}^{N} P_j\, c_j{}^2(k)\tau_1 \frac{\partial^2 V_j}{\partial x^2} + \sum_{j=1}^{N} \mu_{1j} \frac{P_j}{\tau_1}(\mathrm{V_j} - \mathrm{V_1}) \\ 0 \\ \frac{1}{T_2}\left[V_{2e}\left({k}/{1+2\delta_2}\right) - V_2\right] + \left(\frac{1+6\delta_2}{2}\right)\sum_{j=1}^{N} P_j\, c_j{}^2(k)\tau_2 \frac{\partial^2 V_j}{\partial x^2} + \sum_{j=1}^{N} \mu_{2j} \frac{P_j}{\tau_2}(\mathrm{V_j} - \mathrm{V_2}) \\ . \\ . \\ . \\ 0 \\ \frac{1}{T_N}\left[V_{ne}\left({k}/{1+2\delta_N}\right) - V_N\right] + \left(\frac{1+6\delta_N}{2}\right)\sum_{j=1}^{N} P_j\, c_j{}^2(k)\tau_N \frac{\partial^2 V_j}{\partial x^2} + \sum_{j=1}^{N} \mu_{Nj} \frac{P_j}{\tau_N}(\mathrm{V_j} - \mathrm{V_N}) \end{bmatrix}$$

Quasi-linear form of the model to identify the Eigen value of the system

Quasi-linear form:

$$U_t + \boldsymbol{A}(\boldsymbol{U})U_x = S(U)$$

Jacobian matrix form:

$$\boldsymbol{A}(\boldsymbol{U}) = \begin{bmatrix} V_1 & K_1 & 0 & 0 & \cdot\ \cdot\ \cdot & 0 & 0 \\ 0 & V_1 + p_1(2\delta_1+1)\mathrm{KV}_1(K)' & 0 & p_2(2\delta_2+1)KV_2(K)' & \cdot\ \cdot\ \cdot & 0 & p_N(2\delta_N+1)KV_N(K)' \\ 0 & 0 & V_2 & K_2 & \cdot\ \cdot\ \cdot & 0 & 0 \\ 0 & p_1(2\delta_1+1)KV_1(K)' & 0 & V_2 + p_2(2\delta_2+1)KV_2(K) & \cdot\ \cdot\ \cdot & 0 & p_N(2\delta_N+1)\mathrm{KV}_N(K)' \\ \cdot & \cdot & \cdot & \cdot & & \cdot & \cdot \\ \cdot & \cdot & \cdot & \cdot & \cdot\ \cdot\ \cdot & \cdot & \cdot \\ \cdot & \cdot & \cdot & \cdot & & \cdot & \cdot \\ 0 & 0 & 0 & 0 & \cdot\ \cdot\ \cdot & V_N & K_N \\ 0 & p_1(2\delta_1+1)KV_1(K)' & 0 & p_2(2\delta_2+1)\mathrm{KV}_2(K) & \cdot\ \cdot\ \cdot & 0 & V_N + p_N(2\delta_N+1)KV_N(K) \end{bmatrix}$$

Jacobian Matrix and Eigen values

Jacobian Matrix for two vehicles classes

$$A(U) = \begin{bmatrix} U_1 & K_1 & 0 & 0 \\ 0 & U_1 + Kp_1(2\delta_1+1)U_1(K)' & 0 & Kp_2(2\delta_2+1)U_2(K)' \\ 0 & 0 & U_2 & K_2 \\ 0 & Kp_1(2\delta_1+1)U_1(K)' & 0 & U_2 + Kp_2(2\delta_2+1)U_2(K)' \end{bmatrix}$$

Eigen values of the system of equation

$\lambda_1 = U_1,$ $\lambda_2 = U_2,$

$$\lambda_3 = \frac{1}{2}\left\{U_1 + U_2 + (1+2\delta_1)Kp_1V_1[K]' + (1+2\delta_2)Kp_2U_2[K]' - \sqrt{\begin{matrix}(-U_1 - U_2 - (1+2\delta_1)Kp_1U_1[K]' - (1+2\delta_2)Kp_2U_2[K]')^2 - 4(U_1U_2 + (1+ \\ 2\delta_1)Kp_1U_2U_1[K]' + (1+2\delta_2)Kp_2U_1U_2[K]')\end{matrix}}\right\}$$

$$\lambda_4 = \frac{1}{2}\left\{U_1 + U_2 + (1+2\delta_1)Kp_1V_1[K]' + (1+2\delta_2)Kp_2U_2[K]' + \sqrt{\begin{matrix}(-U_1 - U_2 - (1+2\delta_1)Kp_1U_1[K]' - (1+2\delta_2)Kp_2U_2[K]')^2 - 4(U_1U_2 + (1+ \\ 2\delta_1)Kp_1U_2U_1[K]' + (1+2\delta_2)Kp_2U_1U_2[K]')\end{matrix}}\right\}$$

Model properties

Property	Proposed Model
Hyperbolacity	√
Anisotropy	√
Over come wrong way travel	√
Linear stability	√
Travelling and shock waves	√
Heterogeneity	√
Non-lane behaviour	√
Driver memory	√

Linear stability analysis

- Small disturbance in the traffic stream due to change in density or speed will be carried by characteristic waves and they moves at a speed of traffic sound speed in a moving co-ordinate system i.e. $(x - V_0 t, t)$.

The roots of the equation are:

$$\omega_{1,2} = -\frac{1}{2T}\Big[\big(-i + iT\beta\gamma^2 + Tc_1\gamma + Tc_2) \\ \pm\sqrt{(i - iT\beta\gamma^2 - Tc_1\gamma - Tc_2)^2 - 4T(ic\gamma - T\beta c_2 i\gamma^3 + Tc_1c_2\gamma^2)}\Big]$$

The neutral stability criteria $\Omega = V_e'\left(\frac{k_0}{1+2\delta}\right)\frac{k_0}{1+2\delta} + c_0 = 0$

Effect of two-sided lateral gap on stability of traffic flow

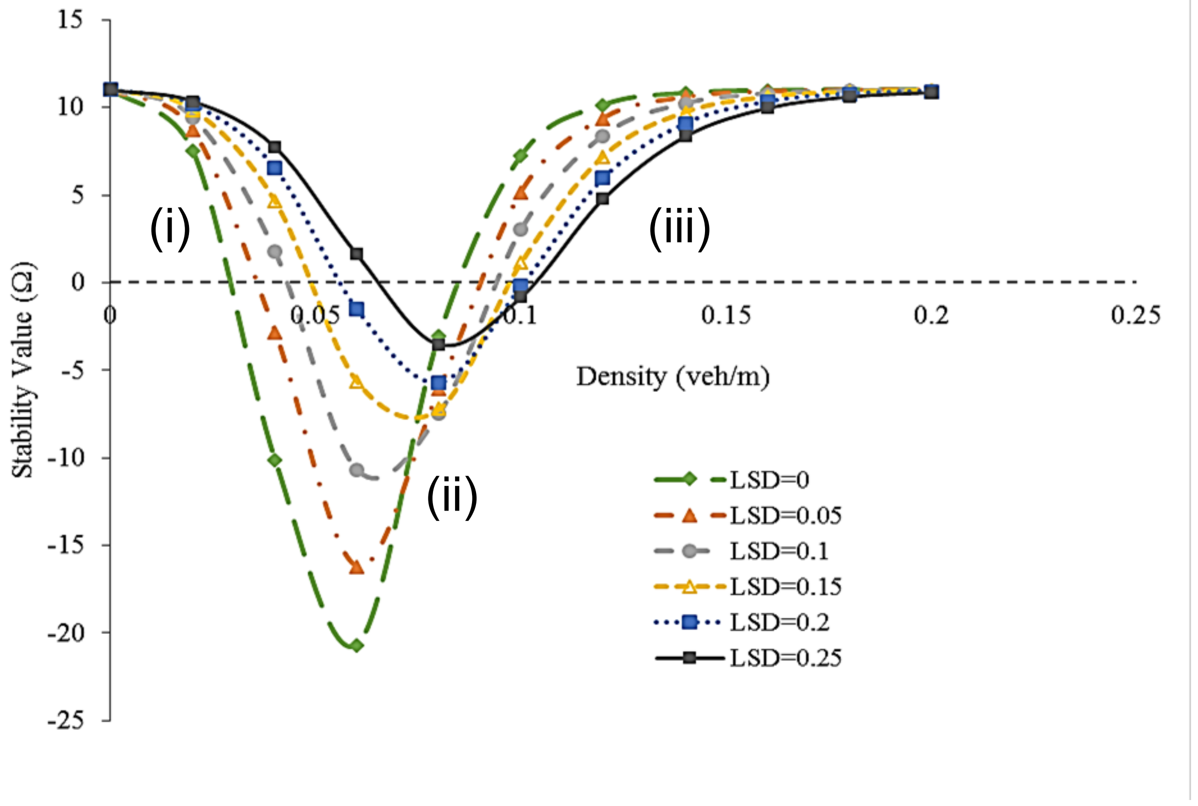

Figure 5: In the figure interval (i) and (iii) represents the stable and metastable regions respectively where perturbation decays either towards downstream or upstream. Interval (ii) represents the unstable region where clusters appear.

Calibration and validation of NLHT model- Methodology

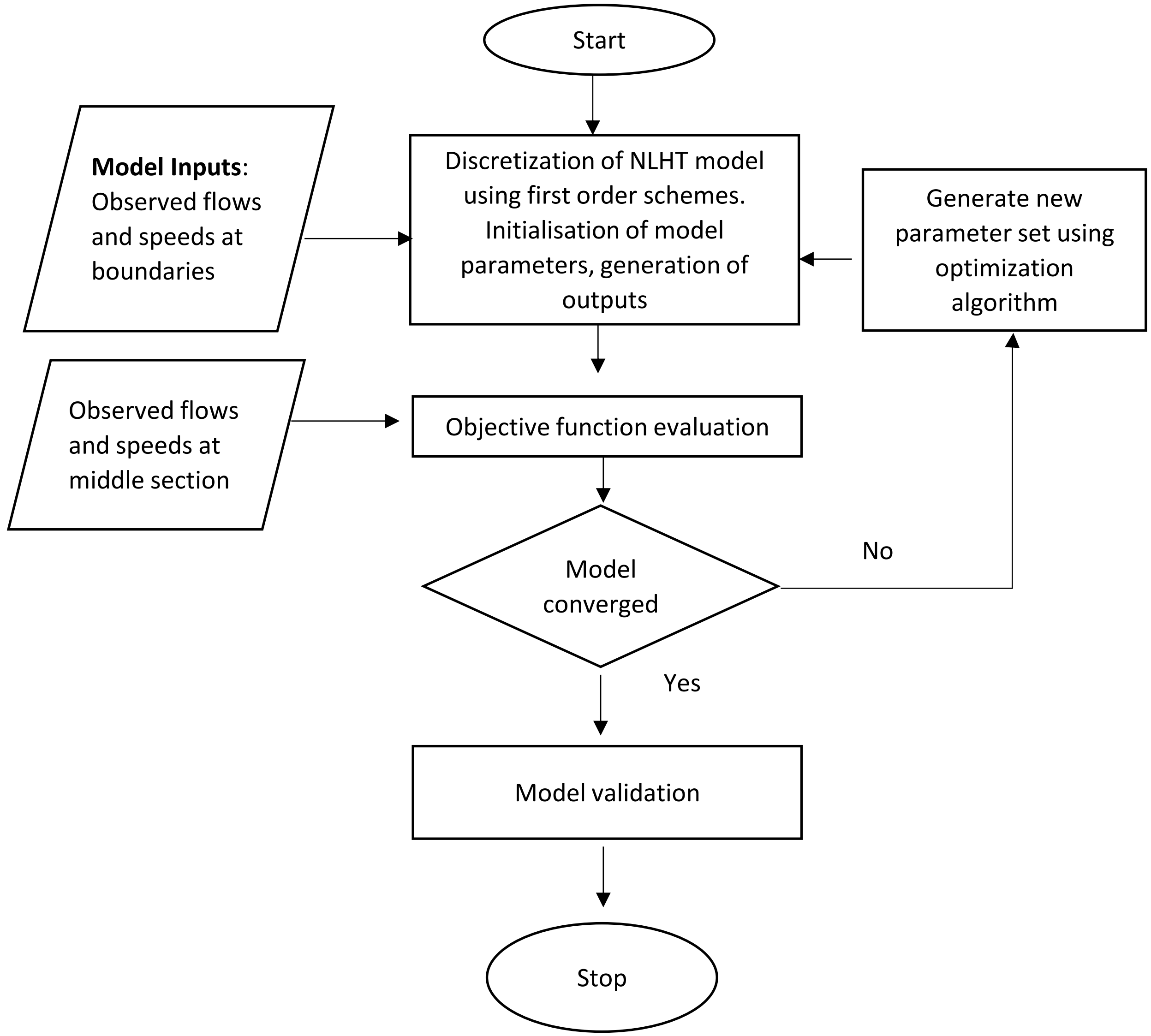

Performance evaluation function

- Root mean square error (RMSE) value of flows and speeds is used as performance evaluation function in estimating parameters

$$PI = \sqrt{\frac{1}{N}\sum_{\mathrm{i}=1}^{N}[y(i) - y^m(i)]^2} \qquad \text{(iv)}$$

❖ Here, PI=performance index, N=number of values, y (i)= vector represent the observed quantities, y^m (i)= vector represents the estimated quantities

Numerical Scheme

- To explore the full potential of the new model and to avoid the numerical instabilities at large gradients, the present study adopted upwind scheme

$$k_{i,m}^{r+1} = k_{i,m}^{r} - \left(\frac{\Delta t}{\Delta x}\right)\left[\left(v_{i,m}^{r}\right)\left(k_{i,m}^{r} - k_{i-1,m}^{r}\right) + k_{i,m}^{r}\left(v_{i+1,m}^{r} - v_{i,m}^{r}\right)\right],$$

$$v_{i,m}^{r+1} = \begin{cases} v_{i,m}^{r} - \left(\frac{\Delta t}{\Delta x}\right)\left(v_{i,m}^{r}\right)\left(v_{i+1,m}^{r} - v_{i,m}^{r}\right) + \left(\frac{\Delta t}{\Delta x}\right)(1+2\delta_m)\sum_{j=1}^{N} P_j c_j(k)\left(V_{i+1,j}^{r} - V_{i,j}^{r}\right) + \\ \frac{\Delta t}{T_m}\left(V_{me}(k_i^{r}) - v_{i,m}^{r}\right) + \sum_{j(\neq m)}^{N} \mu_{mj}\frac{P_j}{\tau_m}\left(v_{i+1,j}^{r} - v_{i,m}^{r}\right) + \\ \left(\frac{\Delta t}{\Delta x^2}\right)\left(\frac{1+6\delta_m}{2}\right)\sum_{j=1}^{N} P_j c_j^2(k)\tau_m\left(v_{i+2,j}^{r} - 2v_{i+1,j}^{r} + v_{i,j}^{r}\right) \text{ if } v_{i,m}^{r} < c_m(k) \\ v_{i,m}^{r} - \left(\frac{\Delta t}{\Delta x}\right)\left(v_{i,m}^{r}\right)\left(v_{i,m}^{r} - v_{i-1,m}^{r}\right) + \left(\frac{\Delta t}{\Delta x}\right)(1+2\delta_m)\sum_{j=1}^{N} P_j c_j(k)\left(v_{i,j}^{r} - v_{i-1,j}^{r}\right) + \\ \frac{\Delta t}{T_m}\left(V_{me}(k_i^{r}) - v_{i,m}^{r}\right) + \sum_{j(\neq m)}^{N} \mu_{mj}\frac{P_j}{\tau_m}\left(v_{i,j}^{r} - v_{i-1,m}^{r}\right) + \\ \left(\frac{\Delta t}{\Delta x^2}\right)\left(\frac{1+6\delta_m}{2}\right)\sum_{j=1}^{N} P_j c_j^2(k)\tau_m\left(v_{i-2,j}^{r} - 2v_{i-1,j}^{r} + v_{i,j}^{r}\right) \text{ if } v_{i,m}^{r} > c_m(k). \end{cases}$$

where $k_{i,m}{}^{r}, v_{i,m}{}^{r}$ are density and speed of the m^{th} class vehicle at point (x_i, t^r), respectively, $k_i{}^{r}$ is the total density of vehicles at point (x_i, t^r) on the road.

Location and Traffic data

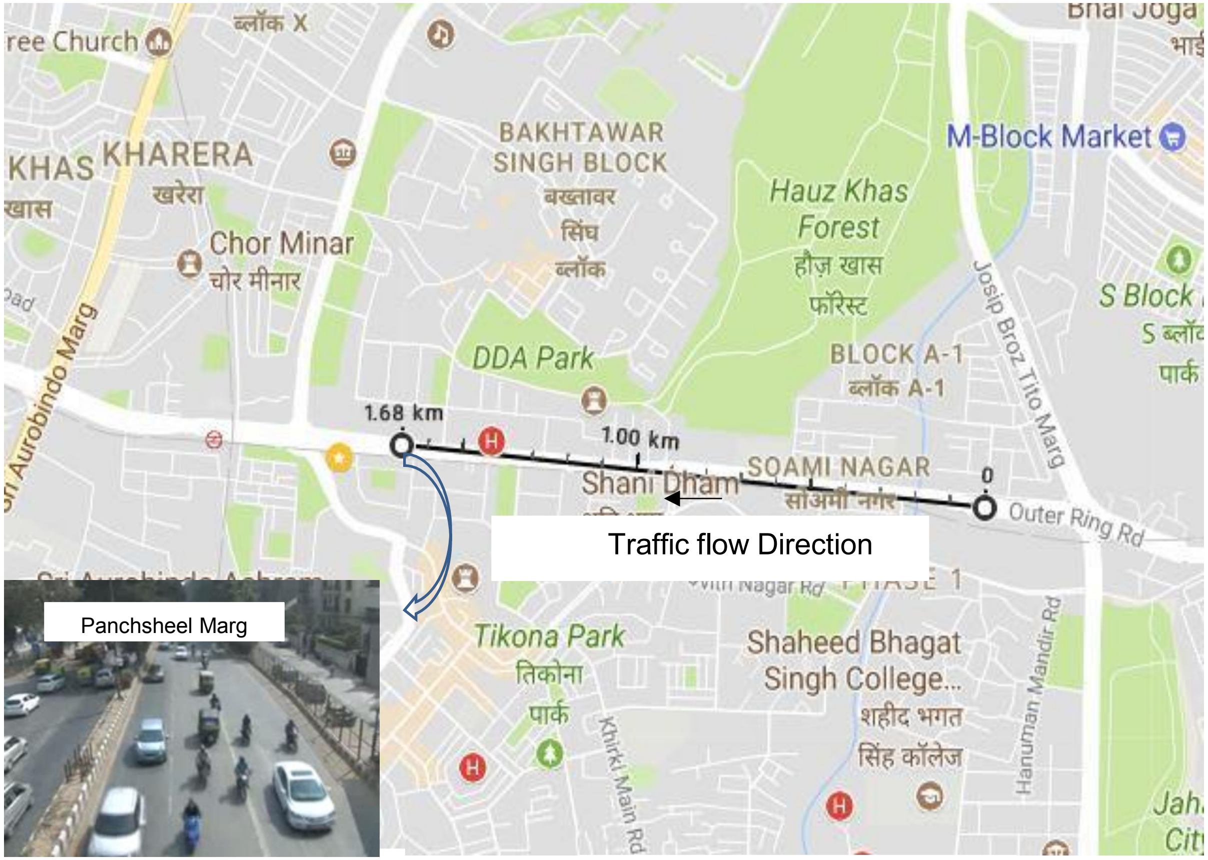

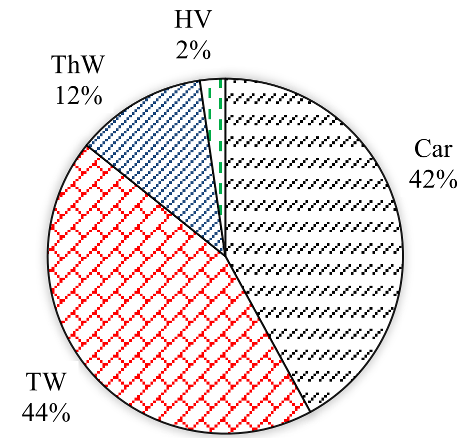

Fig 6: Vehicle composition for four different vehicle classes

Panchsheel Marg

Traffic flow Direction

GDN Marg

Location 3 — Section length = 720 m, width=11 m — **Location 2** — Section length=960 m, width= 11 m — **Location 1**

- Data related to flows and speeds are collected for 1 h 30 min using video camera
- Flows and speeds are extracted and aggregated for every 5 sec interval
- Density is estimated using fundamental relationship of traffic flow

Optimization algorithms

- To solve non-linear, non-differentiable and discontinuous problem, derivative free optimization algorithms are used to calibrate the model parameters. Specifically,

1. Evolutionary algorithms such as Genetic Algorithm (GA) and Simulated Annealing (SA)
2. Hybrid search algorithm such as GA + Nelder Mead
3. Direct search algorithm such as Pattern Search (PS)

Development of traffic flow model, optimization algorithm and calibration procedure are performed in MATLAB 2015 a.

Optimization algorithm parameters

GA:

- Population size - 200, fitness scaling – rank, selection rate- stochastic uniform
- Reproduction: elite count- 0.05*population size = 10, cross over fraction- 0.8*190 = 152, remaining 38 are mutating individuals
- mutation – Gaussian function, cross over – using random binary vector

SA:

- Annealing function – fast annealing (take random steps with size proportional to temperature)
- Reannealing interval -100, temp. update function – exponential temp (temp decreases as 1/log(iteration))
- Initial temp =100 , acceptance probability function = SA acceptance

Optimization algorithm parameters

PS: It is a poll and search method. Pattern search polls the mesh points and mesh size will decrease or increase after a successful / unsuccessful poll

- Poll – Generalised pattern search positive basis 2N
- Search – complete search (all the points must be searched at each iteration)
- Mesh size – minimum 1 and maximum infinity
- Expansion factor -2 and contraction factor - 0.5

Calibrated parameters from GA

Vehicle Type	Model Parameters and Cost function value									
	K_{jam} (veh/km)	V_f (km/h)	a	b	E	Th	T	t	δ	**RMSE, Iterations, Computational time**
Car		64.8	4	1	10.3	2.1	9.99	5.98	0.10	**13.24%**
MTW	240	61.2	4	1	11.0	1.5	9.99	5.99	0.11	**229**
MThW		50.4	4	1	11.2	1.5	9.99	5.99	0.12	**22.58 min**
HV		50.4	4	1	11.0	1.5	9.99	5.98	0.12	

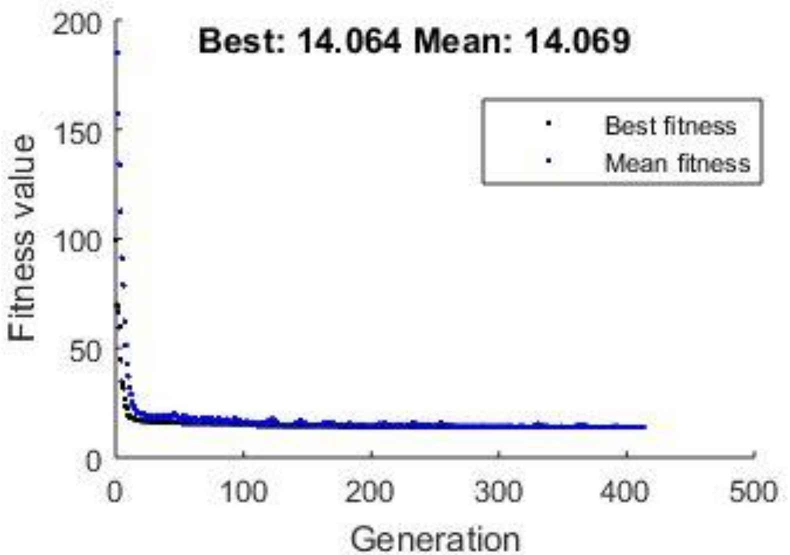

Fig 7: Calibration run 1

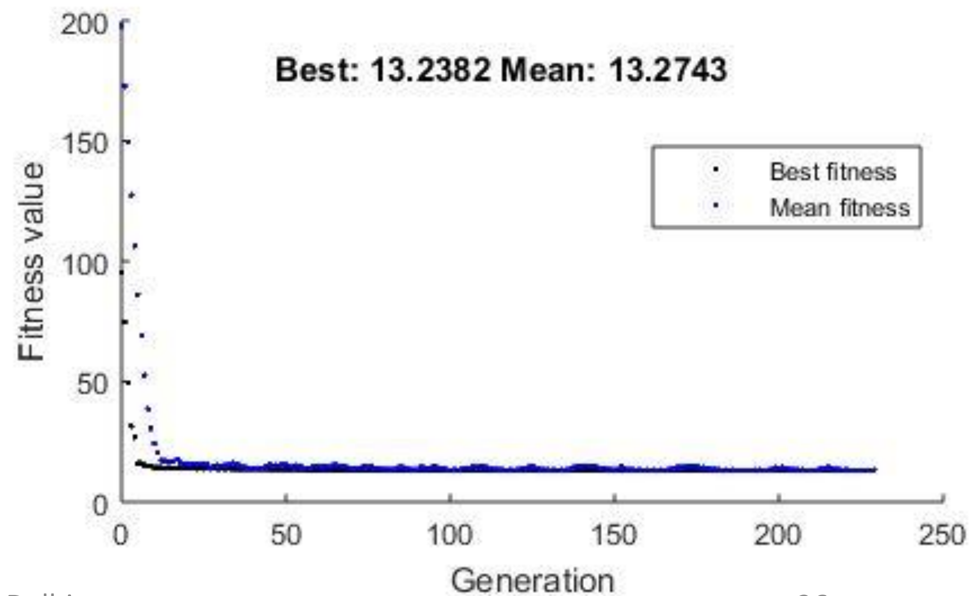

Fig 8:Calibration run 2

Calibrated parameters from GA + Nelder-Mead (Hybrid)

Vehicle Type	Model Parameters and Cost function value									
	K_{jam} (veh/km)	V_f (km/h)	a	b	E	Th	T	t	δ	**RMSE, Iterations, Computational time**
Car	240	63.0	4	1	11.20	1.8	10.2	5.99	0.1	**13.20%** **291** **20.31 min**
MTW		61.0	4	1	10.22	1.5	9.98	5.99	0.1	
MThW		49.2	4	1	10.20	1.5	10.0	5.99	0.1	
HV		49.2	4	1	10.22	1.6	9.99	5.99	0.1	

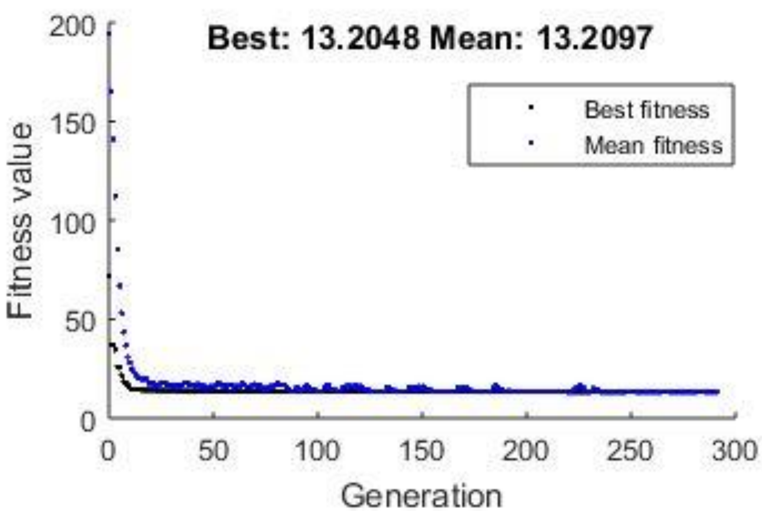

Fig 9: Calibration run 1

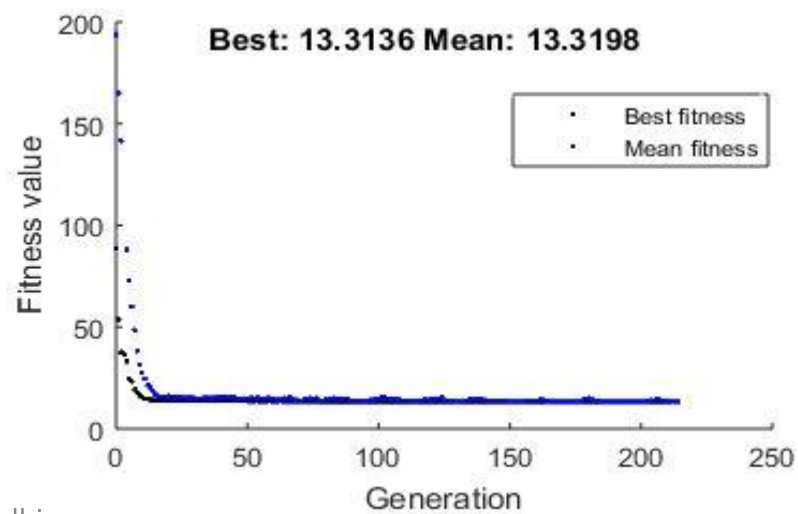

Fig 10: Calibration run 2

Calibrated parameters from Pattern search

Vehicle Type	Model Parameters and Cost function value									
	K_{jam} (veh/km)	V_f (km/h)	a	b	E	Th	T	t	Δ	RMSE, Iterations, Computational time
Car	240	63.4	4	1	10.5	1.5	10	6	0.1	13.19% 224 2.55 min
MTW		60.1	4	1	10.3	1.5	10	6	0.1	
MThW		49.2	4	1	10.4	1.5	10	6	0.1	
HV		49.2	4	1	10.4	1.5	10	6	0.1	

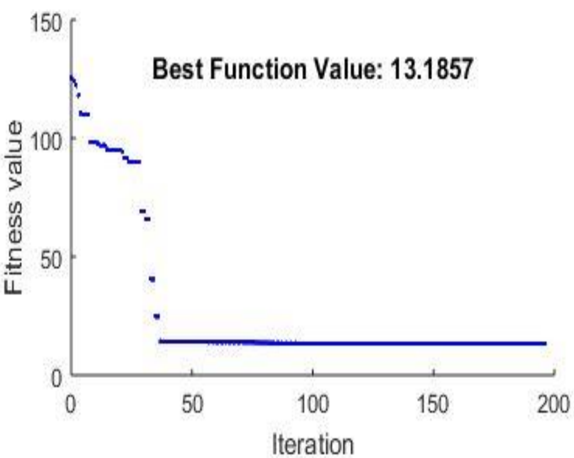

Fig 11: Calibration run 1

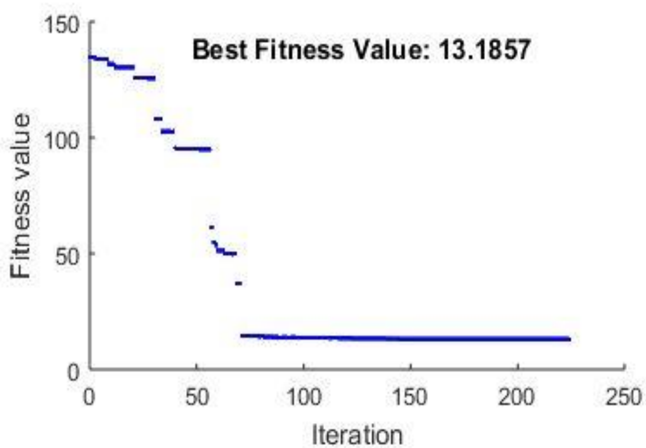

Fig 12: Calibration run 2

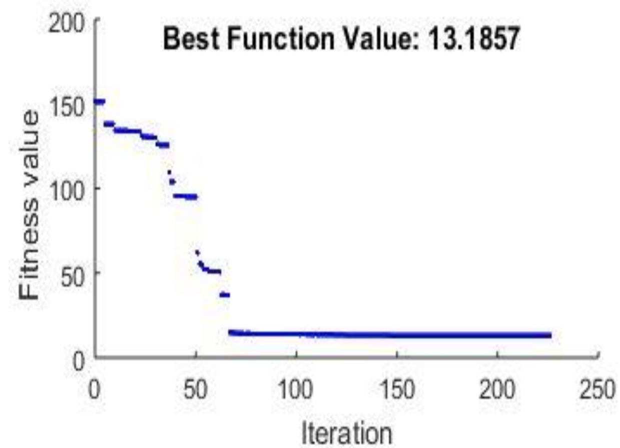

Fig 13: Calibration run 3

Calibrated parameters from simulated annealing

Vehicle Type	Model Parameters and Cost function value									
	K_{jam} (veh/km)	V_f (km/h)	a	b	E	Th	T	t	δ	**RMSE, Iterations, Computational time**
Car	360	76.248	4.2	1	10.2	1.5	8.51	2.40	0.10	**20.701%** **15,340** **16.24 min**
MTW		82.08	4.1	1	10.2	1.5	7.23	2.39	0.10	
MThW		53.712	4.0	1	10.2	1.5	7.86	3.00	0.22	
HV		45.40356	4.0	1	10.2	1.5	8.68	2.75	0.24	

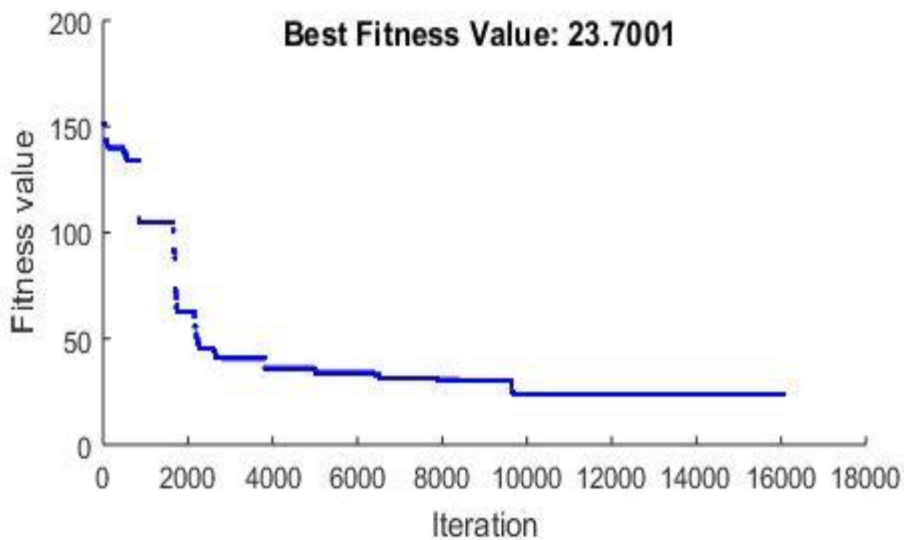

Fig 14: Calibration run 1

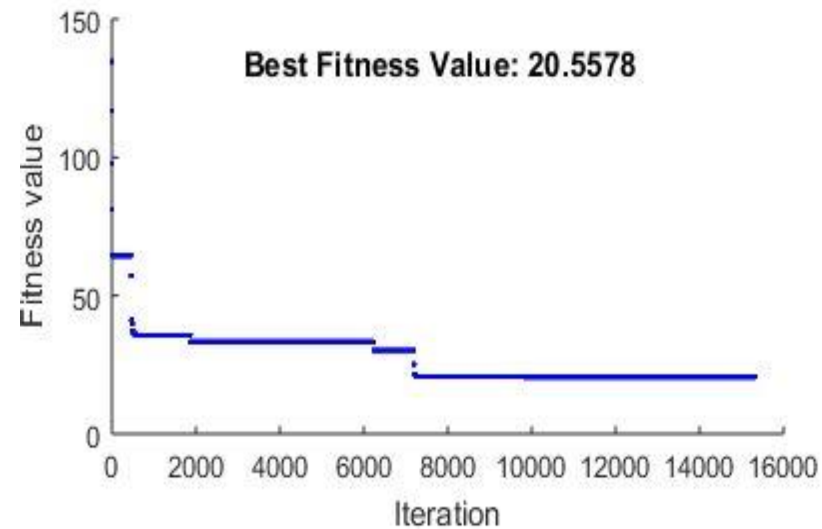

Fig 15: Calibration run 2

Some observations

Calibration Algorithm	Algorithm performance		
	RMSE	Iterations	Computational time (min)**
Genetic Algorithm	13.24%	229	22.58
Hybrid search (GA+ fmincon trust region reflective algorithm)	13.20%	291	20.31
Simulated Annealing (SA)	20.70%	15340	16.24
Pattern Search	13.19%	224	**2.55**

**Desktop computer with 3.10 GHZ CPU and 8 GB of RAM

Validation results- Observed vs. Estimated FD

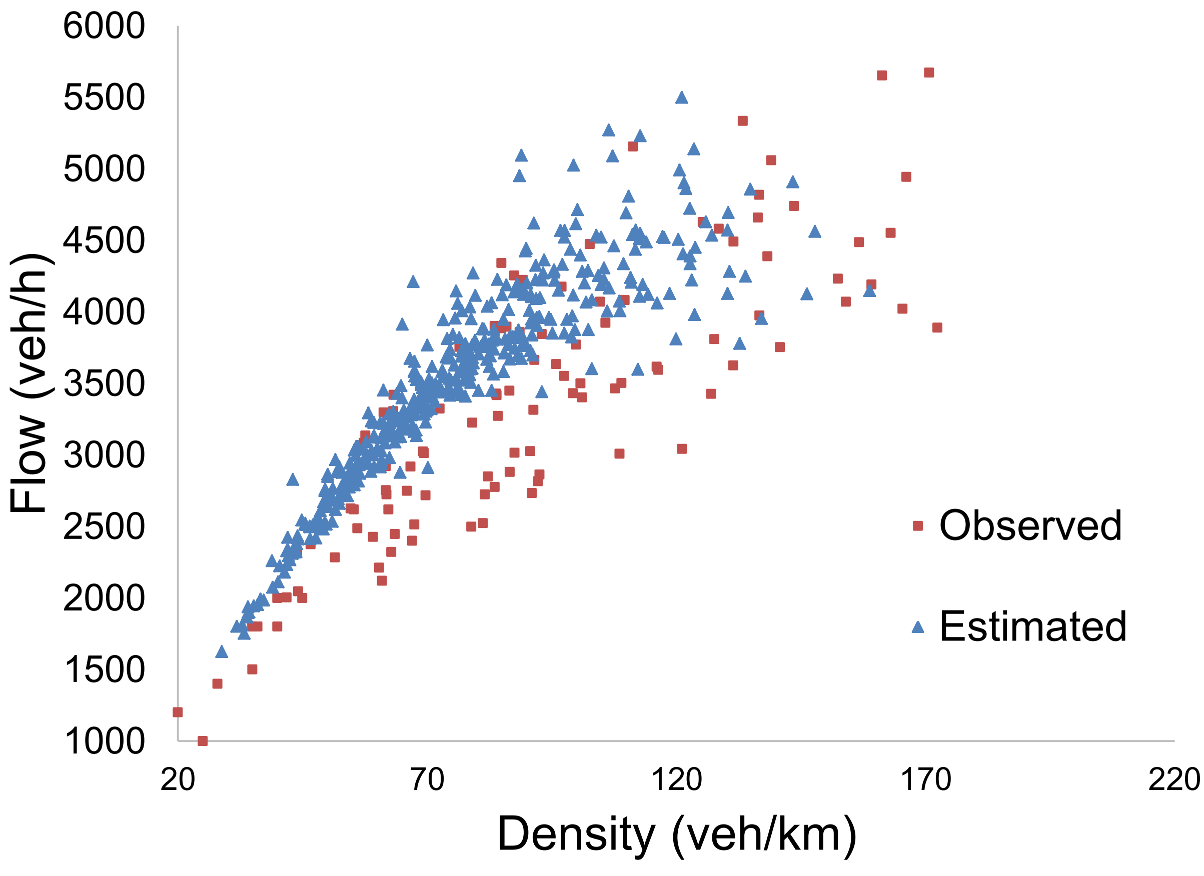

Fig 16: Flow-Density relationship of traffic stream

Local cluster effect

- The proposed model can describe the instantaneous occurrence of traffic jams due to the small disturbances in traffic stream known as **local cluster effect** [Kerner et al. (1995), Hermann and Kerner (1998)]
- The effect of two-sided lateral gap (δ) on spontaneous occurrences of traffic perturbation such as stop-and-go and local clusters due to small changes in traffic density are evaluated

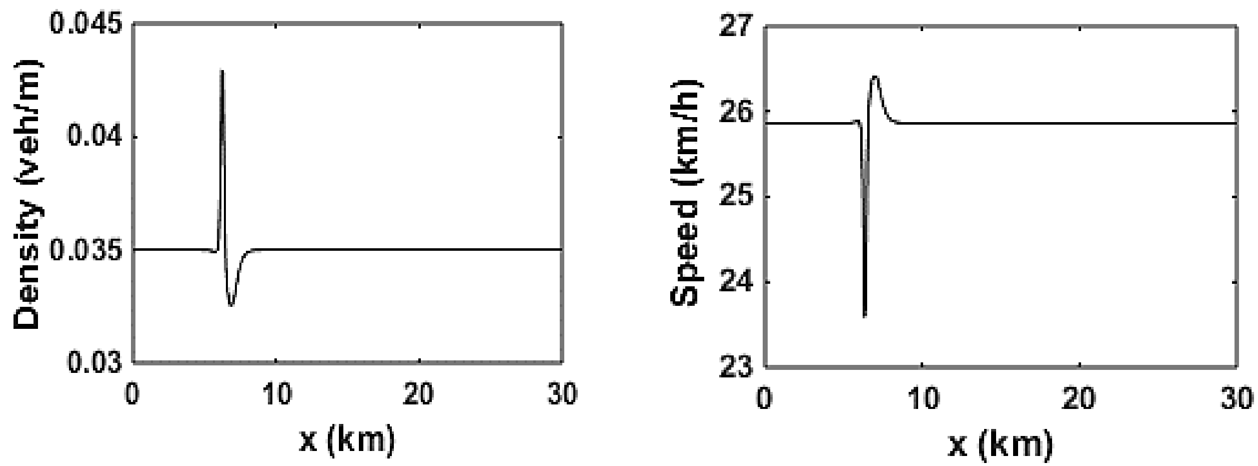

(a) (b)

Figure 17: Initial perturbation of traffic (a) density and (b) speed

Traffic conditions and equilibrium equation

- The numerical simulations will be carried out to localized perturbation assumed in an initially homogenous traffic environment
- The initial distribution of the density, mean speed of the traffic stream are:

$$\mathrm{K(x,o) = K_0 + \Delta K(x), x \in [0,L]\ ,\ V(x,o) = V_{KK}(K(x,o)), x \in [0,L]}$$

Here $\Delta K(x)$ is the localized perturbation caused due to the sudden stopping of vehicles, unexpected changing of lanes etc. (Figure 4).

$$\mathrm{\Delta K(x) = \Delta K_0 \left\{ \cosh^{-2}\left[\frac{160}{L}\left(x - \frac{5L}{16}\right)\right] - \frac{1}{4}\cosh^{-2}\left[\frac{40}{L}\left(x - \frac{11L}{32}\right)\right]\right\}}$$

Here L is the circumference of the circular road section under consideration. In this study, we assume L=30 km as a circumference of a ring road. Periodic boundary conditions used for the numerical simulation are:

$$\mathrm{q(0,t) = q(L,t), V(0,t) = V(L,t), \frac{\partial V(0,t)}{\partial x} = \frac{\partial V(L,t)}{\partial x}}$$

Equilibrium equation $V_{KK}(K)$ used for the analysis is:

$$V_{KK}(\mathrm{K}) = V_f \left\{\left[1 + \exp\left(\frac{K/K_j - 0.25}{0.06}\right)\right]^{-1} - 3.72 * 10^{-6}\right\}$$

Phantom Traffic jams

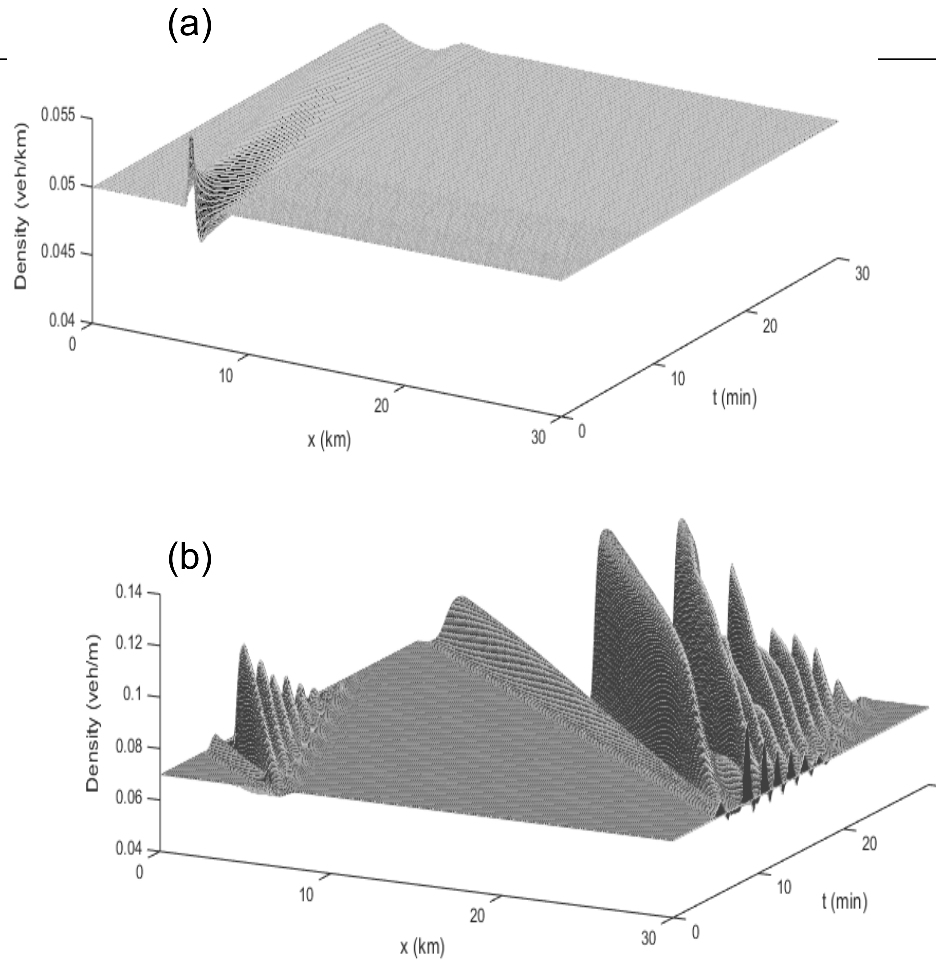

Figure 18: Local cluster effect for localized perturbation of amplitude Δk_0 = 0.01 veh/m and (a) K_0=0.035 veh/m (b) K_0=0.05 veh/m Speed –Gradient (SG) Model (Jiang et al.(2002))

Local cluster phenomenon explained by two sided lateral gap model

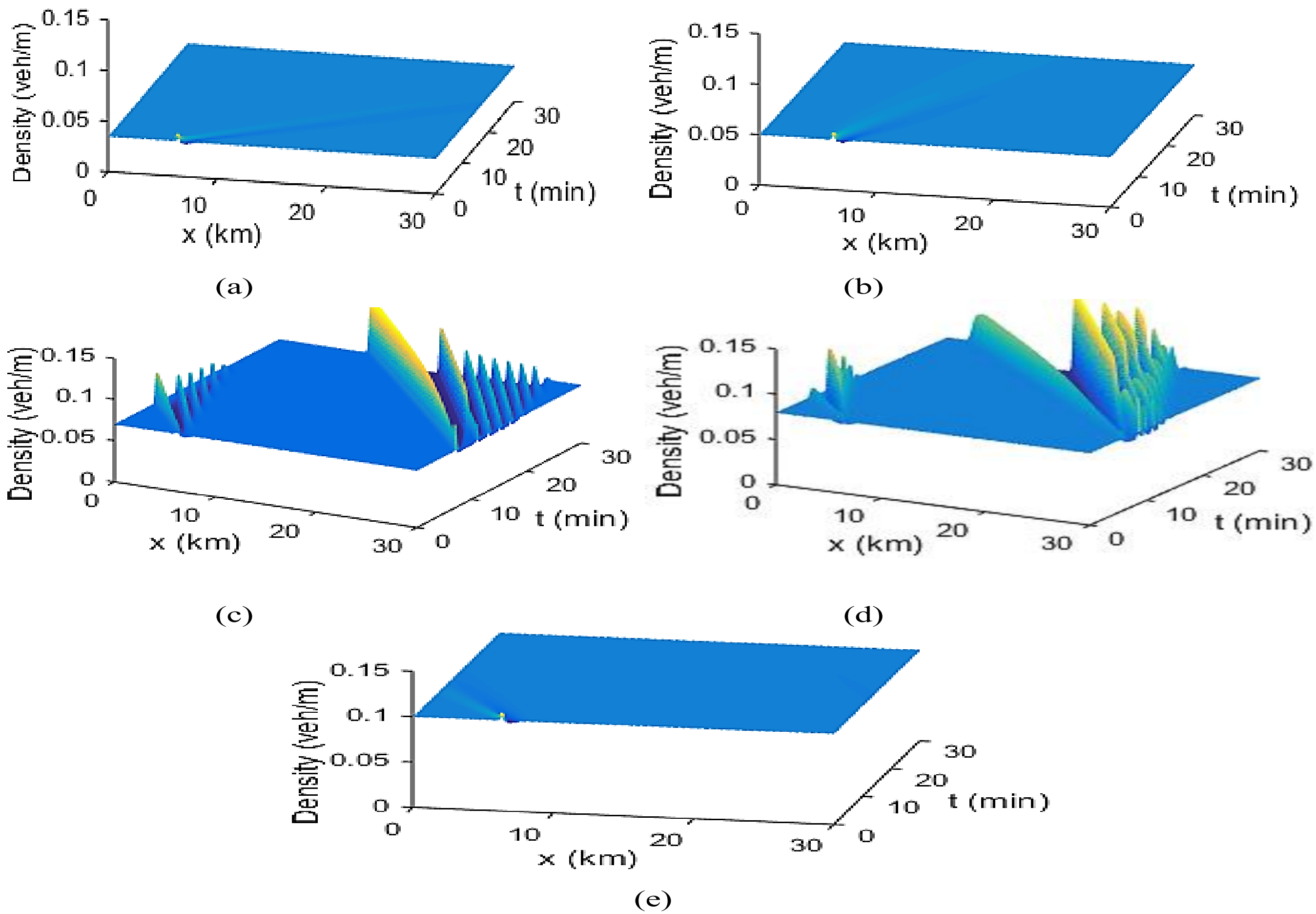

Fig 19: Spatio-temporal evolution of density on a 30 km ring road for 30 min time where a, b, c, d, e are outputs from the two-sided lateral gap model with ρ_0 = 0.035, 0.05, 0.07, 0.08 and 0.10 and amplitude $\Delta\rho_0$=0.01 and δ=0.2

Local cluster phenomenon explained by two sided lateral gap model

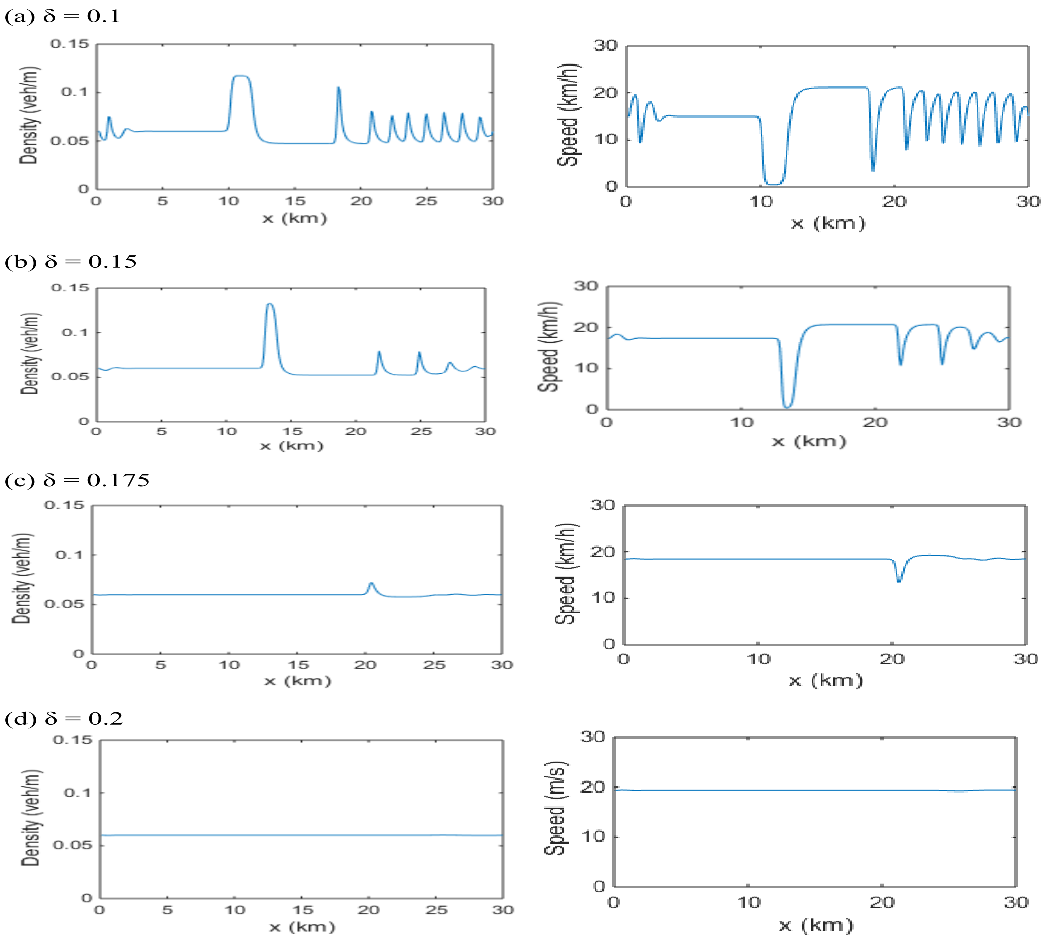

Fig 20: Profile of traffic density and speed on a 30 km ring road at t=1800 sec where $\rho_0 = 0.06$and amplitude $\Delta \rho_0$=0.01

Local cluster phenomenon explained by two sided lateral gap model

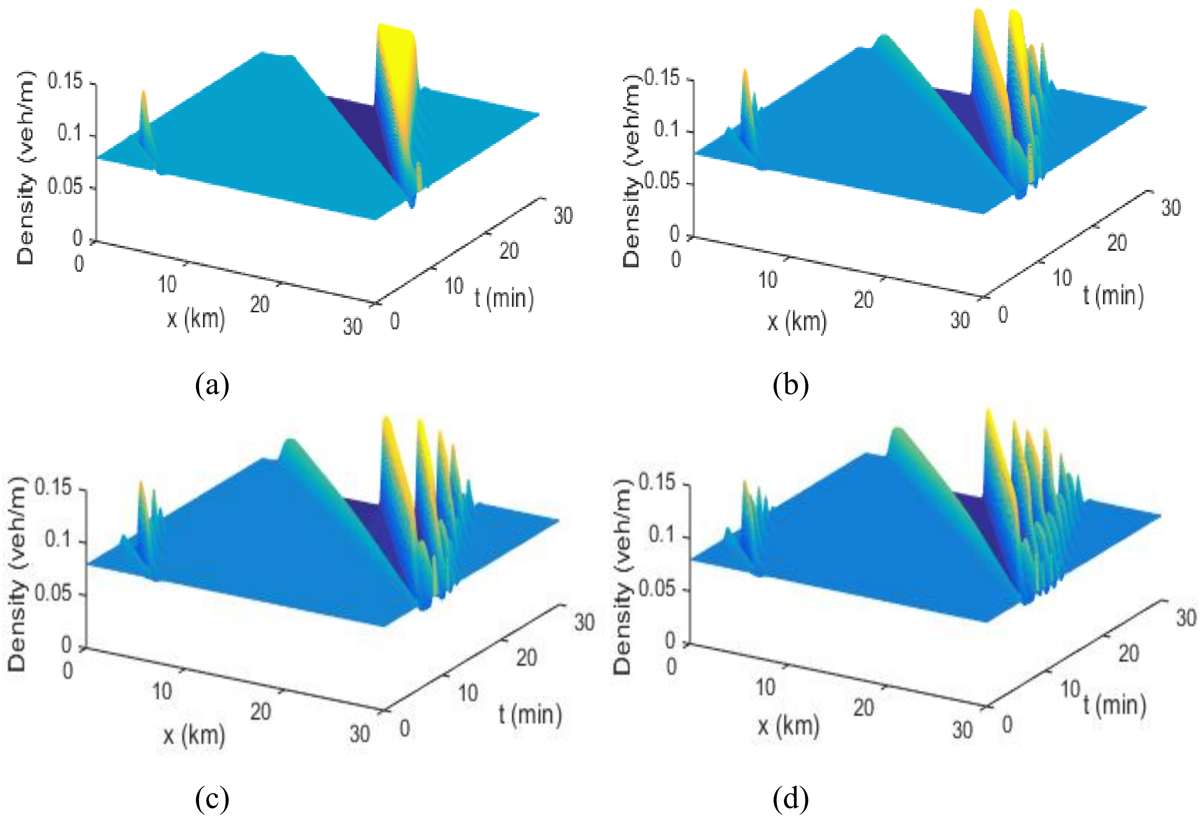

Fig 21: Spatio-temporal evolution of traffic density on a 30 km ring road for 30 min time with $\rho_0 = 0.08$ and amplitude $\Delta\rho_0 = 0.01$ for: (a) $\delta=0.1$ (b) $\delta=0.15$ (c) $\delta=0.175$ (d) $\delta=0.2$

Zhang (2002) anisotropic model vs Two sided lateral gap model

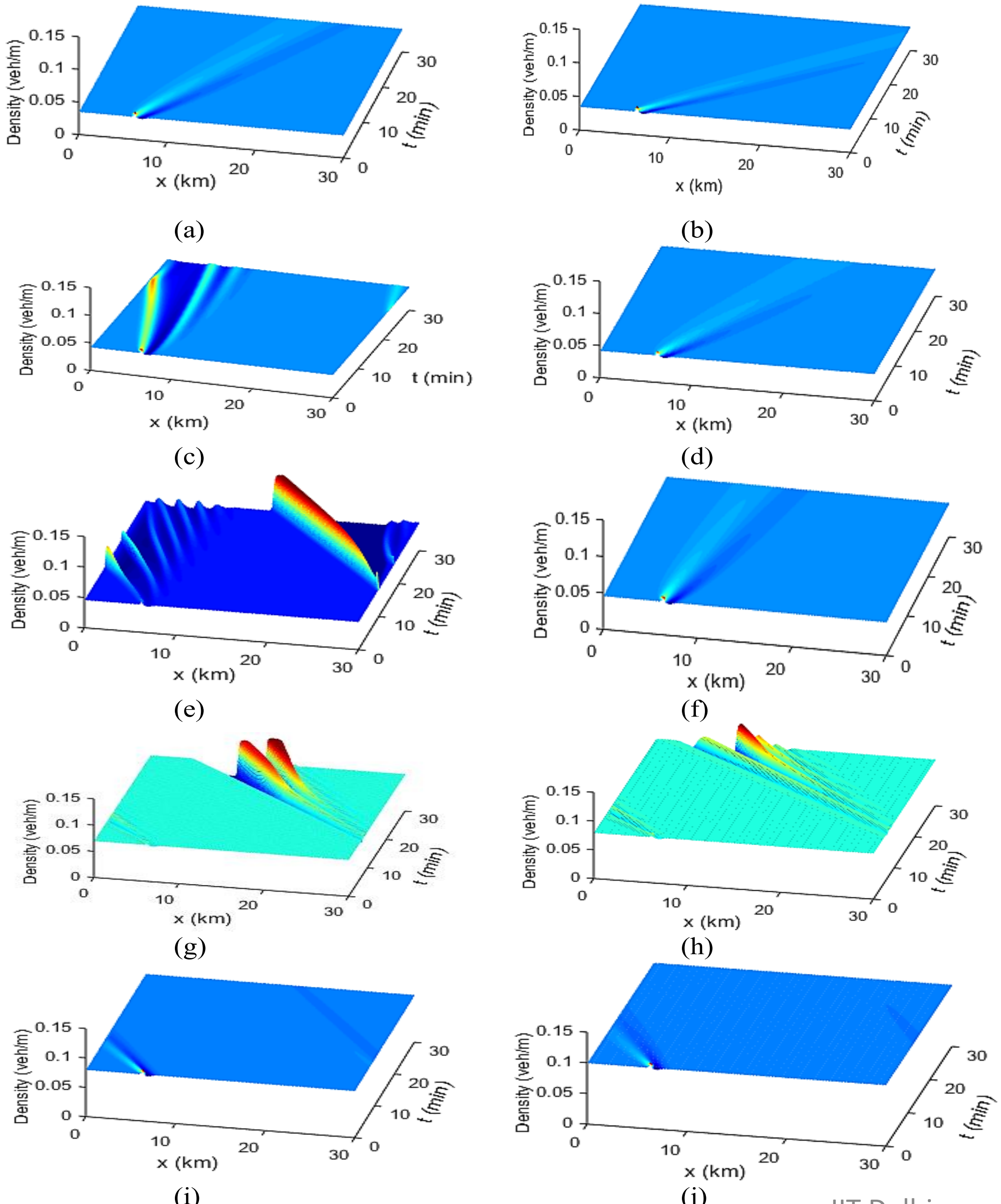

Figure 22: Spatio-temporal evolution of density on a 30 km ring road over 30 min time period.
Where a, c, e, g, i are outputs from the Zhang model (where δ=0) and b, d, f, h, j are the outputs from two sided lateral gap model (where δ=0.1) with
k_0 = 0.035, 0.042, 0.05, 0.07 and 0.10 and amplitude Δ k_0=0.01

One-sided lateral gap model vs Two-sided lateral gap model

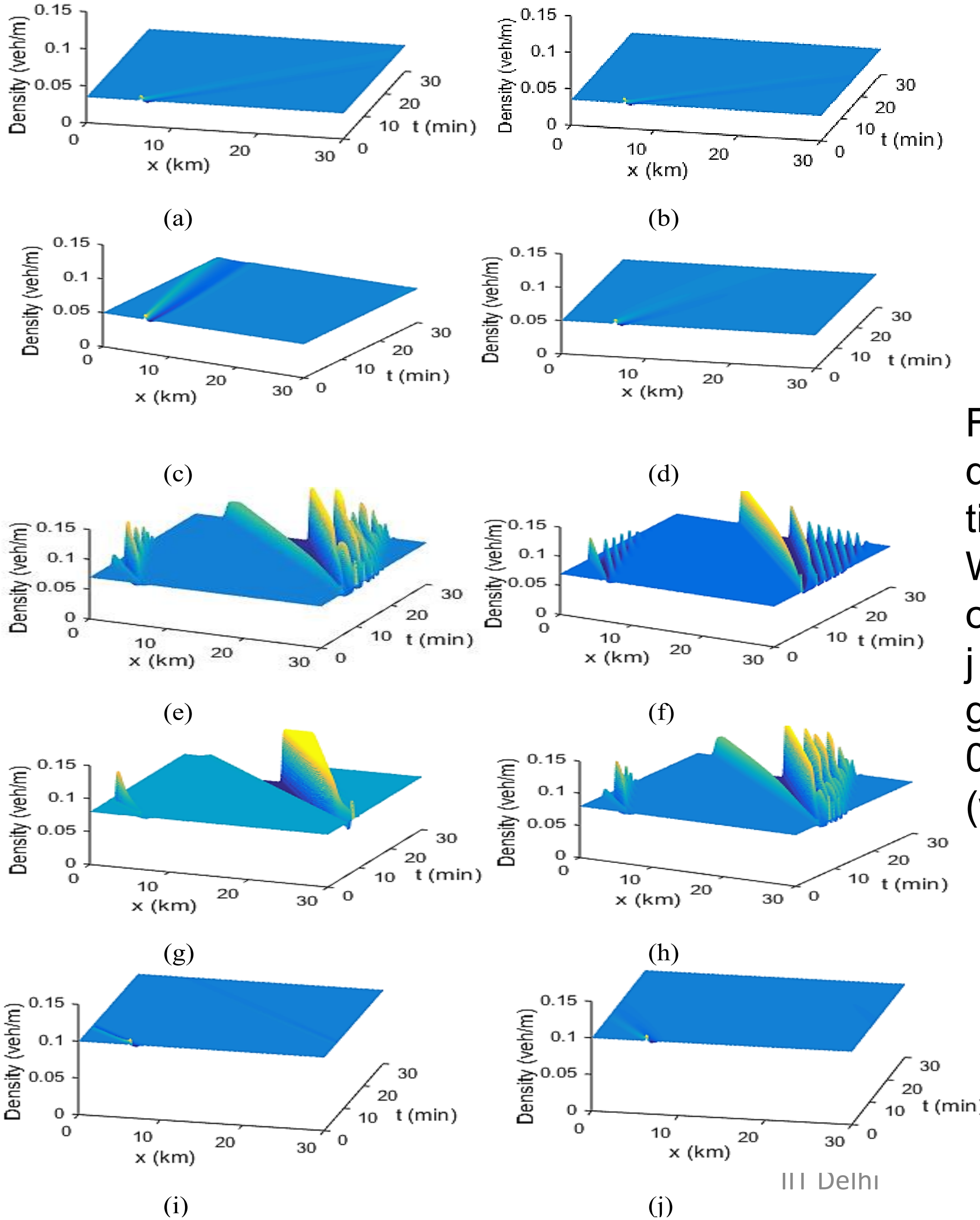

Figure 23: Spatio-temporal evolution of density on a 30 km ring road over 30 min time period.
Where a, c, e, g, i are the outputs from one sided lateral gap model and b, d, f, h, j are the outputs from two-sided lateral gap model with k_0 = 0.035, 0.05, 0.07, 0.08 and 0.10 and amplitude Δk_0=0.01 (where δ=0.2 for both cases)

Summary of the effect of two sided lateral gaps on local clusters

- The results proved that two sided lateral gap model dissipates the small perturbations (local traffic jams) rapidly and it increases the stability region of the traffic flow
- In addition, two-sided lateral gap in the model avoids the sudden deceleration of vehicles and improves the performance of infrastructure
- It is because drivers receive information faster when they maintain off-centeredness with other vehicles and avoids the sudden deceleration.
- Moreover, proposed model can also explain the spontaneous occurrence of traffic jams i.e., called phantom traffic jams.

Local Breakdown effect

- The local breakdown effect is a localized avalanche-like growth in the density and the related decrease in the average speed of vehicles which occurs in a deterministic way in a slightly non-homogeneous traffic flow [Kerner et al. (1994,1996)].

- As a result of such a deterministic effect, traffic jams are self formed even if fluctuations in traffic flow are negligible.

Here assume traffic perturbation: $\Delta \mathrm{K(x)} = \Delta \mathrm{K}_0 cos\left(\frac{2\pi \mathrm{x}}{\mathrm{L}} m\right)$

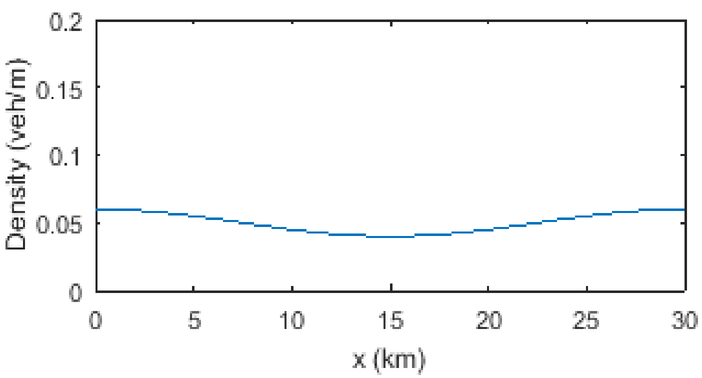

Case (1) : Non-homogeneous traffic density when m=1, ρ0 = 0.05, amplitude $\Delta\rho_0$ = 0.01 at t = 0 sec

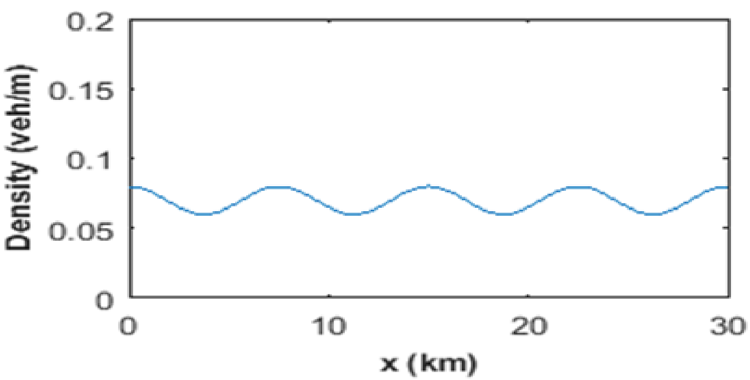

Case (2): Non-homogeneous traffic density when m = 4, ρ0 = 0.07, amplitude $\Delta\rho_0$ = 0.01 at t = 0 sec

Case (1)

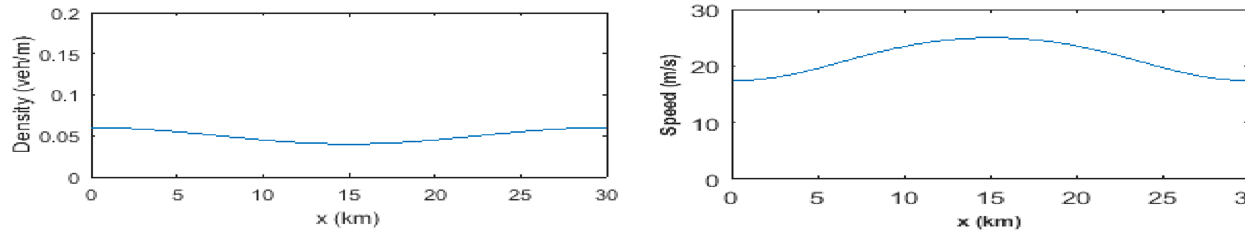

Non-homogeneous traffic density when m = 4, $\rho_0 = 0.07$, amplitude $\Delta\rho_0 = 0.01$ at t = 0 sec

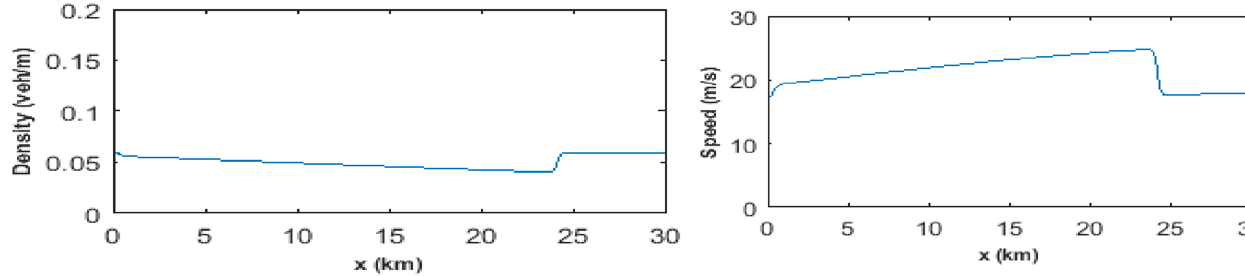

Density and speed profiles on a 30 km ring road at t=720 sec from the two-sided lateral gap model with $\rho_0 = 0.05$, amplitude $\Delta\rho_0 = 0.01$ and δ=0.15

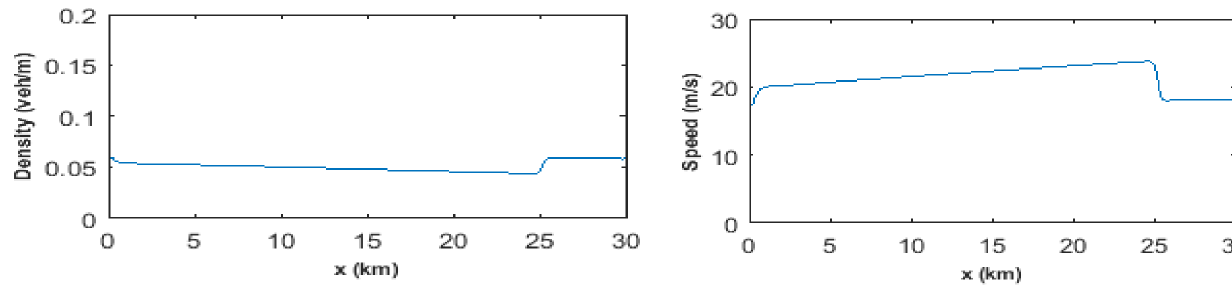

Density and speed profiles on a 30 km ring road at t=1400 sec from the two-sided lateral gap model with $\rho_0 = 0.05$, amplitude $\Delta\rho_0 = 0.01$ and δ=0.15

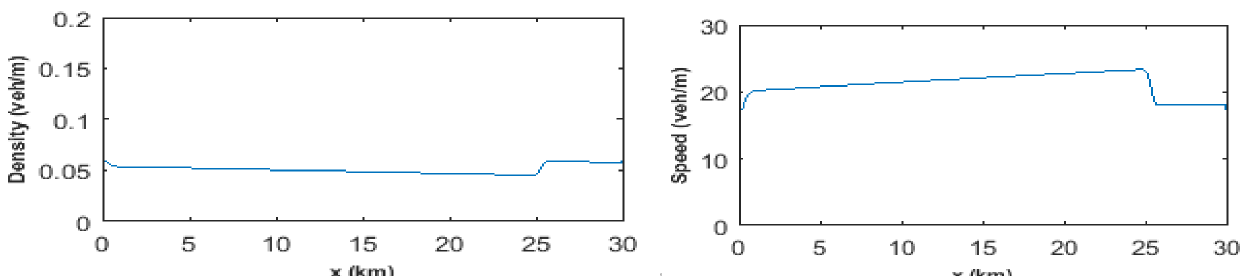

Fig 24: Density and speed profiles on a 30 km ring road at t=1800 sec from the two-sided lateral gap model with $\rho_0 = 0.05$, amplitude $\Delta\rho_0 = 0.01$ and δ=0.15

Case (2)

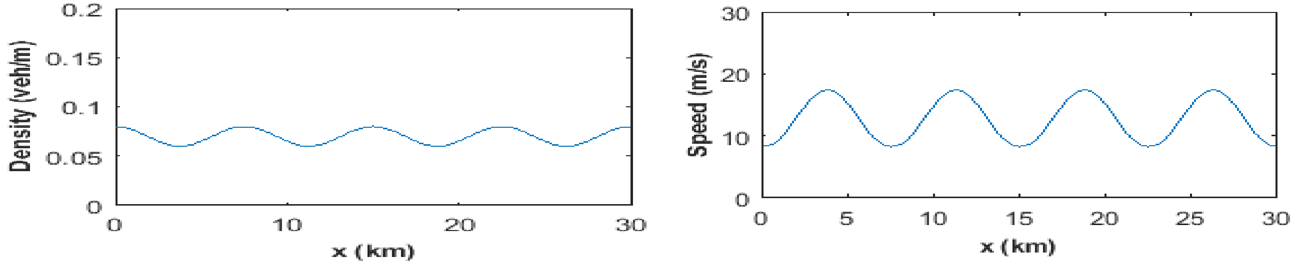

Non-homogeneous traffic density when m = 4, $\rho_0 = 0.07$, amplitude $\Delta\rho_0 = 0.01$ at t = 0 sec

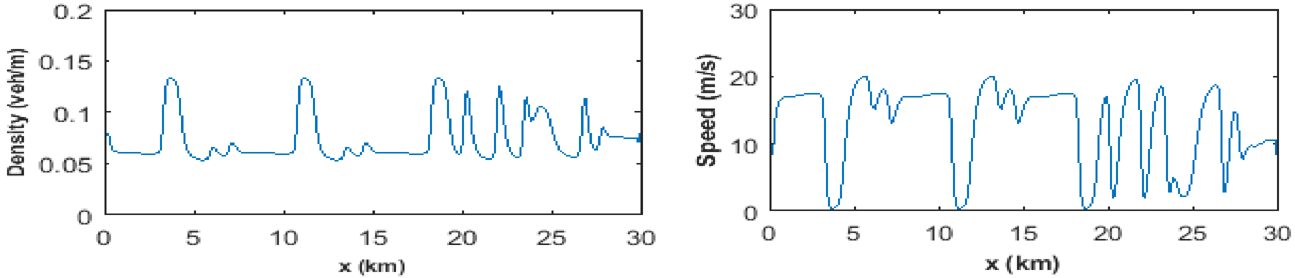

Density and speed profiles on a 30 km ring road at t=720 sec from the two-sided lateral gap model with $\rho_0 = 0.07$, amplitude $\Delta\rho_0 = 0.01$ and δ=0.15

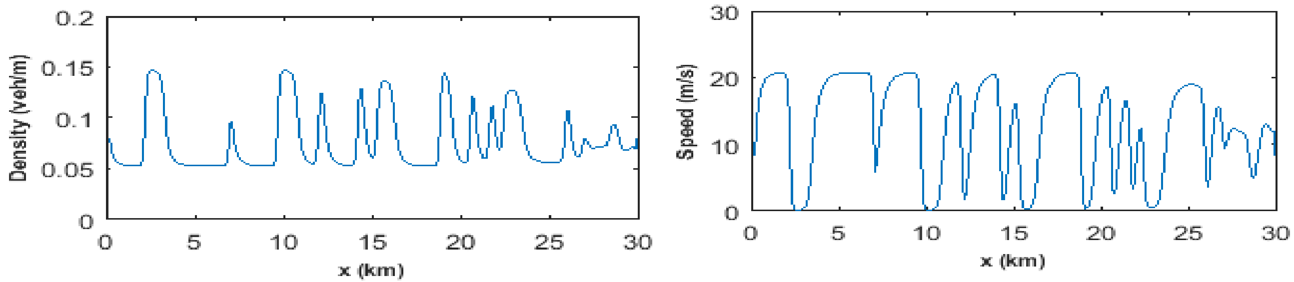

Density and speed profiles on a 30 km ring road at t=1400 sec from the two-sided lateral gap model with $\rho_0 = 0.07$, amplitude $\Delta\rho_0 = 0.01$ and δ=0.15

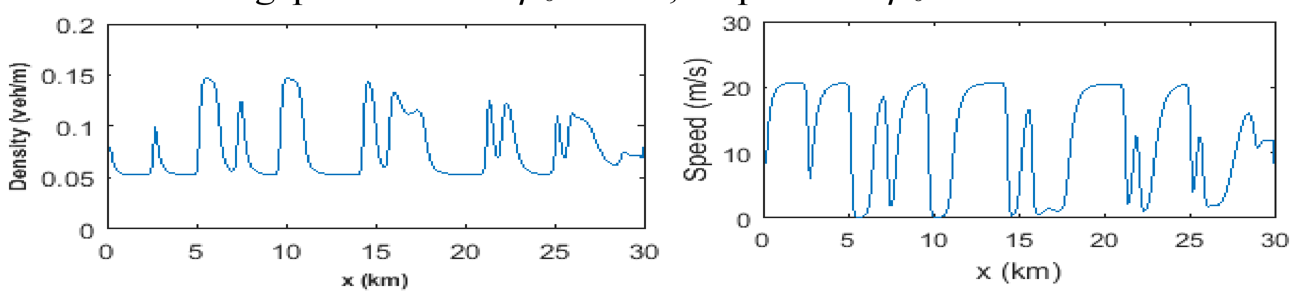

Fig 25: Density and speed profiles on a 30 km ring road at t=1800 sec from the two-sided lateral gap model with $\rho_0 = 0.07$, amplitude $\Delta\rho_0 = 0.01$ and δ=0.15

Outcomes

- At high-density conditions, the number of traffic jams appeared is doubled to that of initial number of perturbations in a slightly non-homogenous environment
- However, slightly less intensity jams also appeared in between these jams at downstream and propagate upwards as time progresses
- At low-density conditions traffic Irrespective of the number of initial perturbation, the perturbations dissipate very quickly and no jams appeared in slightly non-homogeneous environment

Effect of lateral separation distance on Fundamental Diagram (FD)

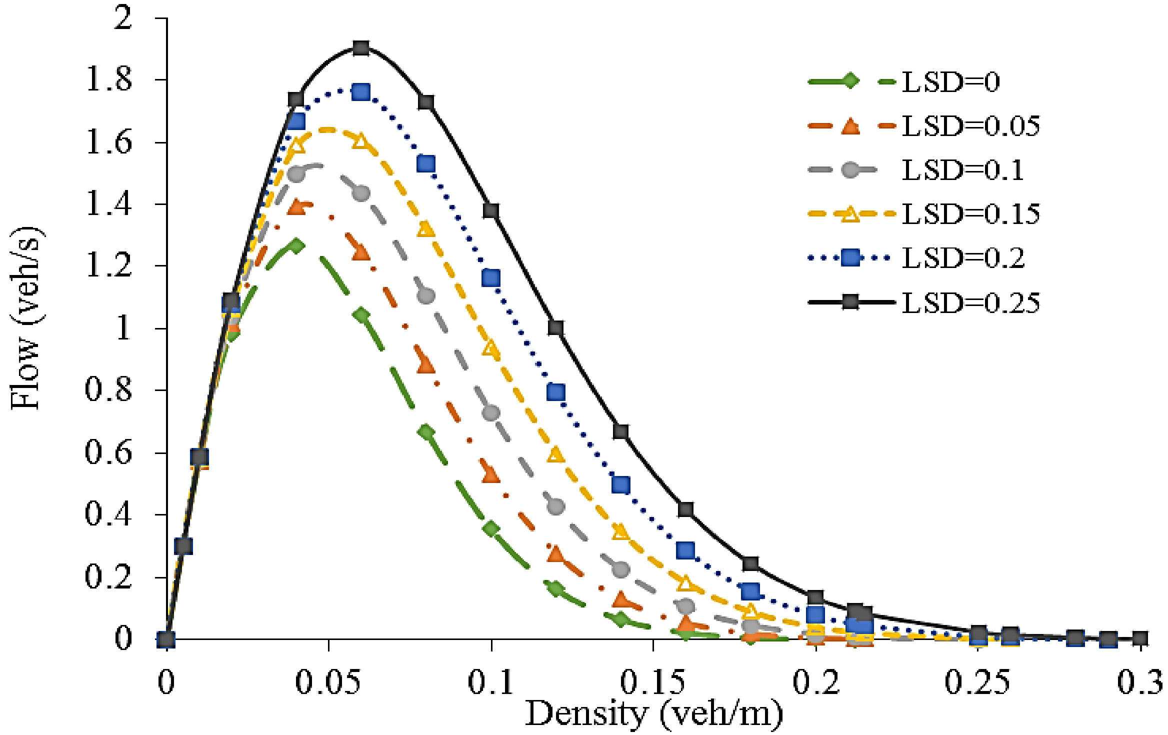

Figure 26: Flow-Density relation

- lateral gap does not affect traffic flow when density is low
- when vehicular density becomes large, the capacity of the traffic stream increases with increasing of two sided lateral gap value
- as density approached jam density, the effect of a two-sided lateral gap on F.D diminishes

Effect of vehicular heterogeneity on fundamental diagram

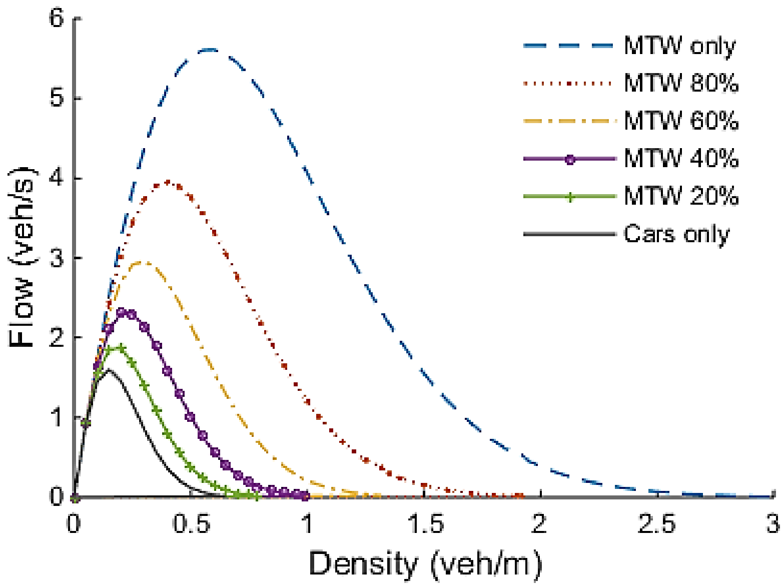

(a)

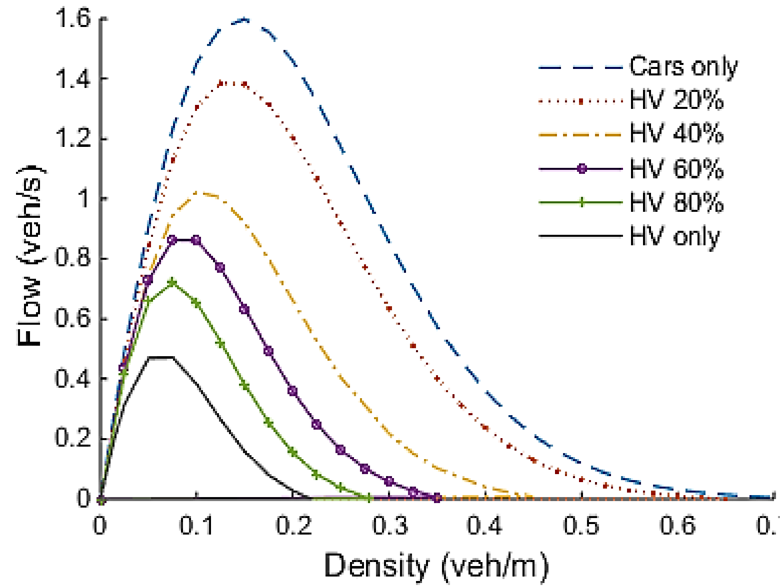

(b)

Figure 27: Effect of (a) MTW and (b) Heavy vehicle proportion on capacity of traffic flow

Exp 1: Traffic break down in non-lane condition

- Road is empty at t = 0 and initial time boundary condition at road entrance is subjected to trapezoidal peak demand

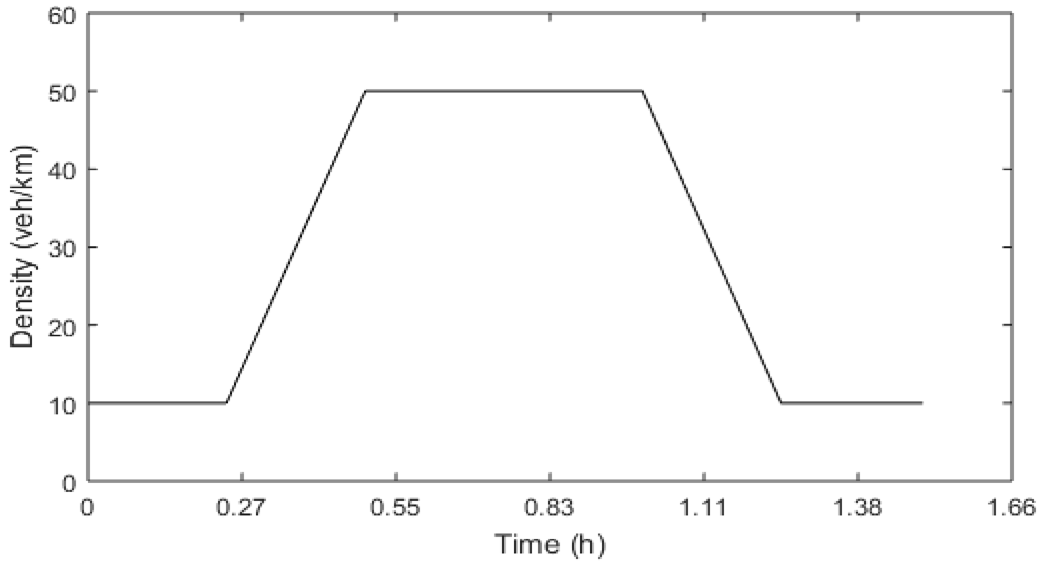

Fig 28: Entry flow at upstream section

- Proportion of vehicle classes as per observed data in the field
- Assumption: incident takes place at downstream and last for 3 min (1.125 h to 1.175 h)

Traffic breakdown scenario

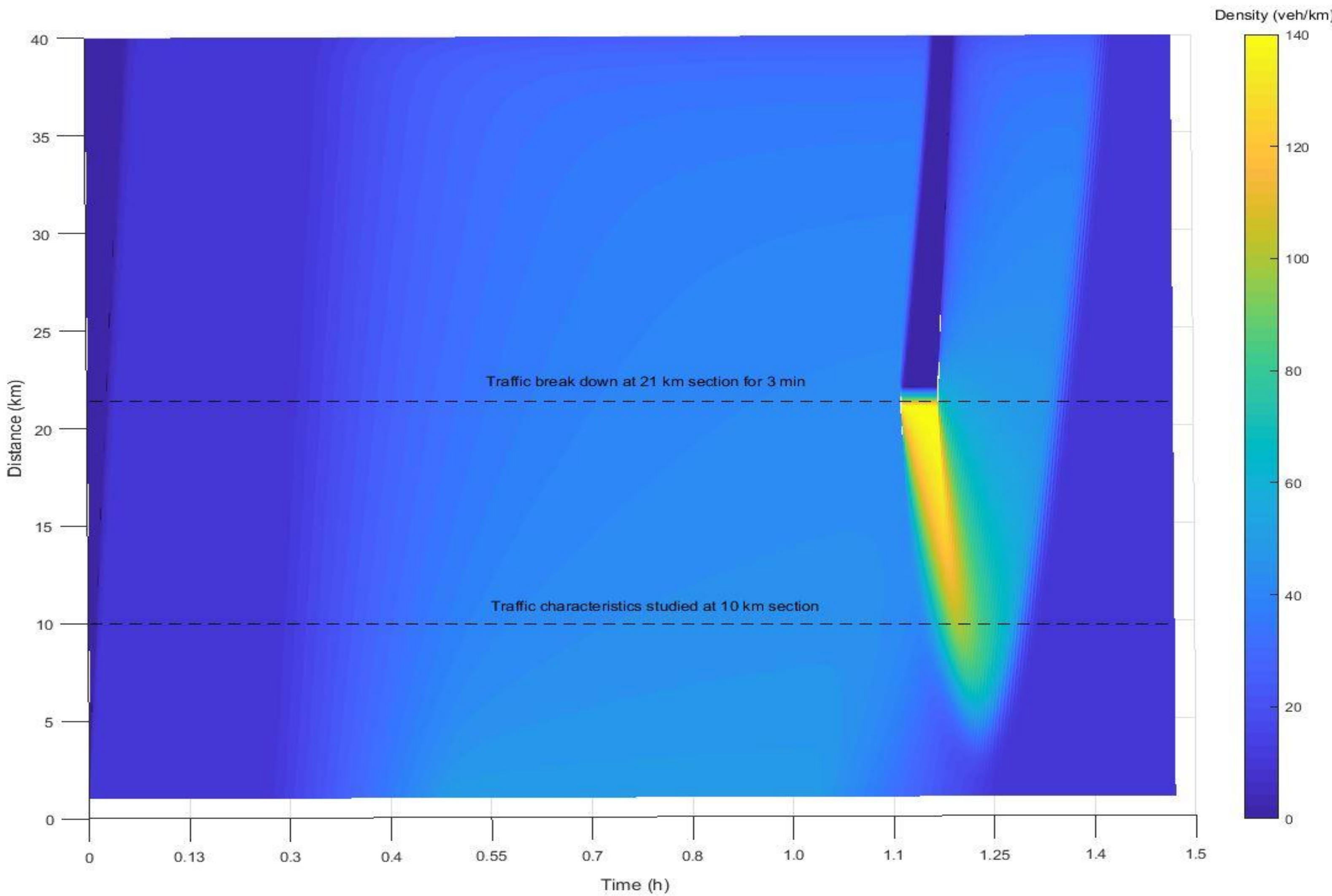

Fig 29: x-t plot showing formation and dissipation of queues due to traffic breakdown

Traffic hysteresis, two-regime capacity condition in non-lane scenario in non-lane traffic

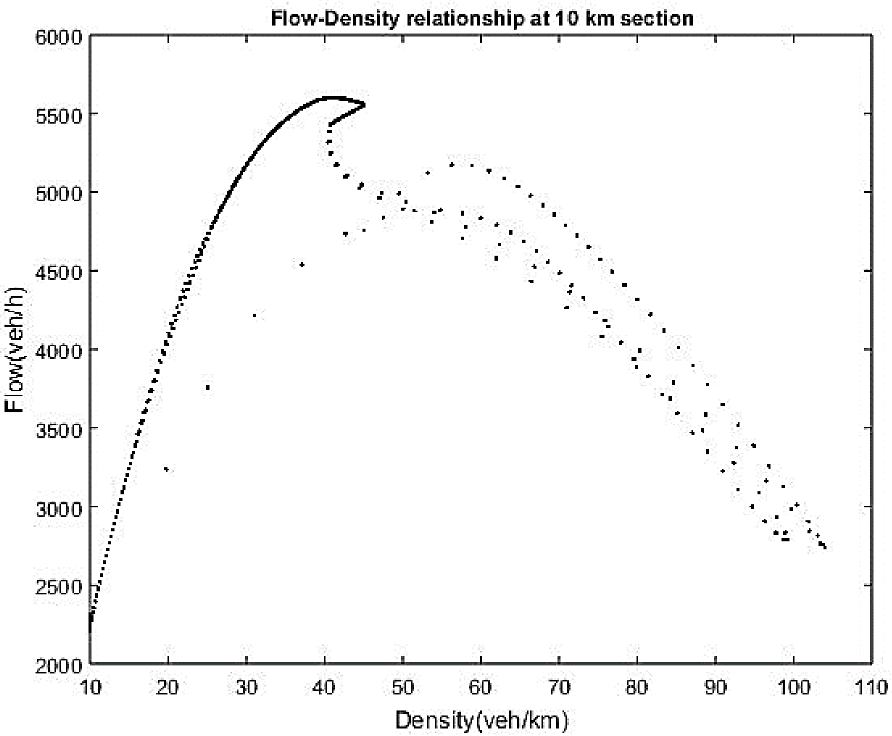

Fig 30: Two-regime capacity condition

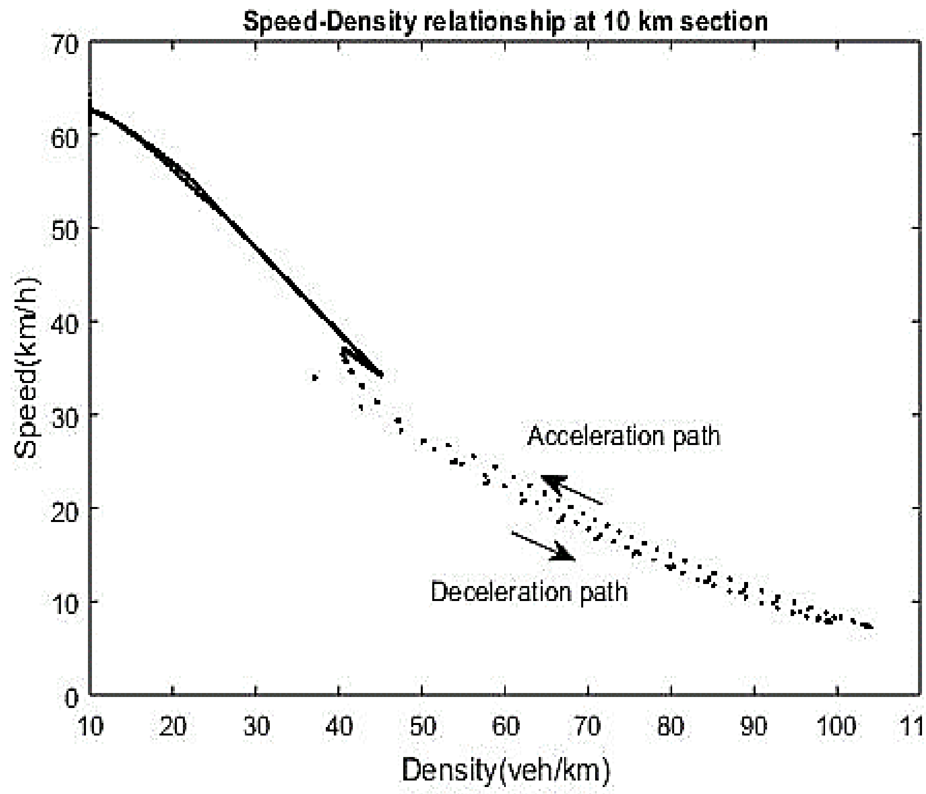

Fig 31: Hysteresis

Exp2: Platoon dispersion characteristics

- Initial density conditions on the road are assumed as per figure below

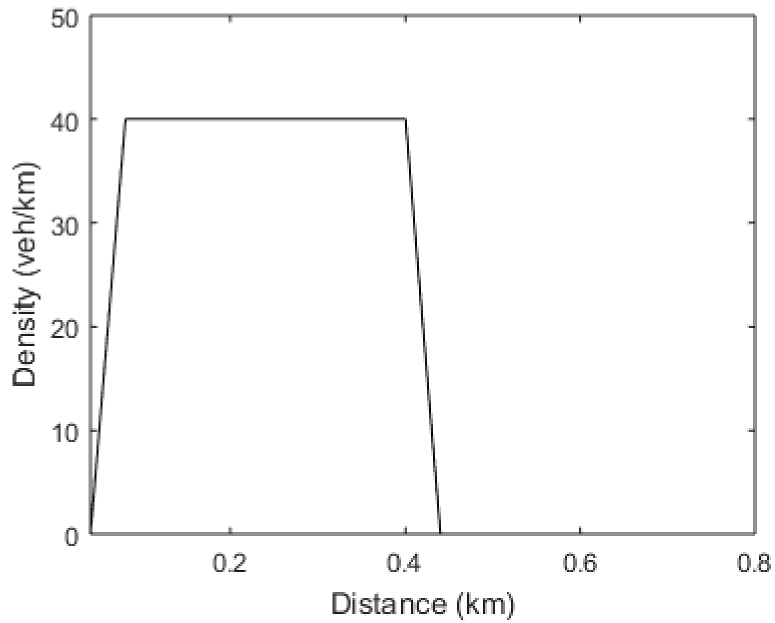

Fig 32: Initial density conditions

- No traffic entered from the upstream and vehicle composition according to the field observations

Platoon dispersion characteristics of heterogeneous traffic

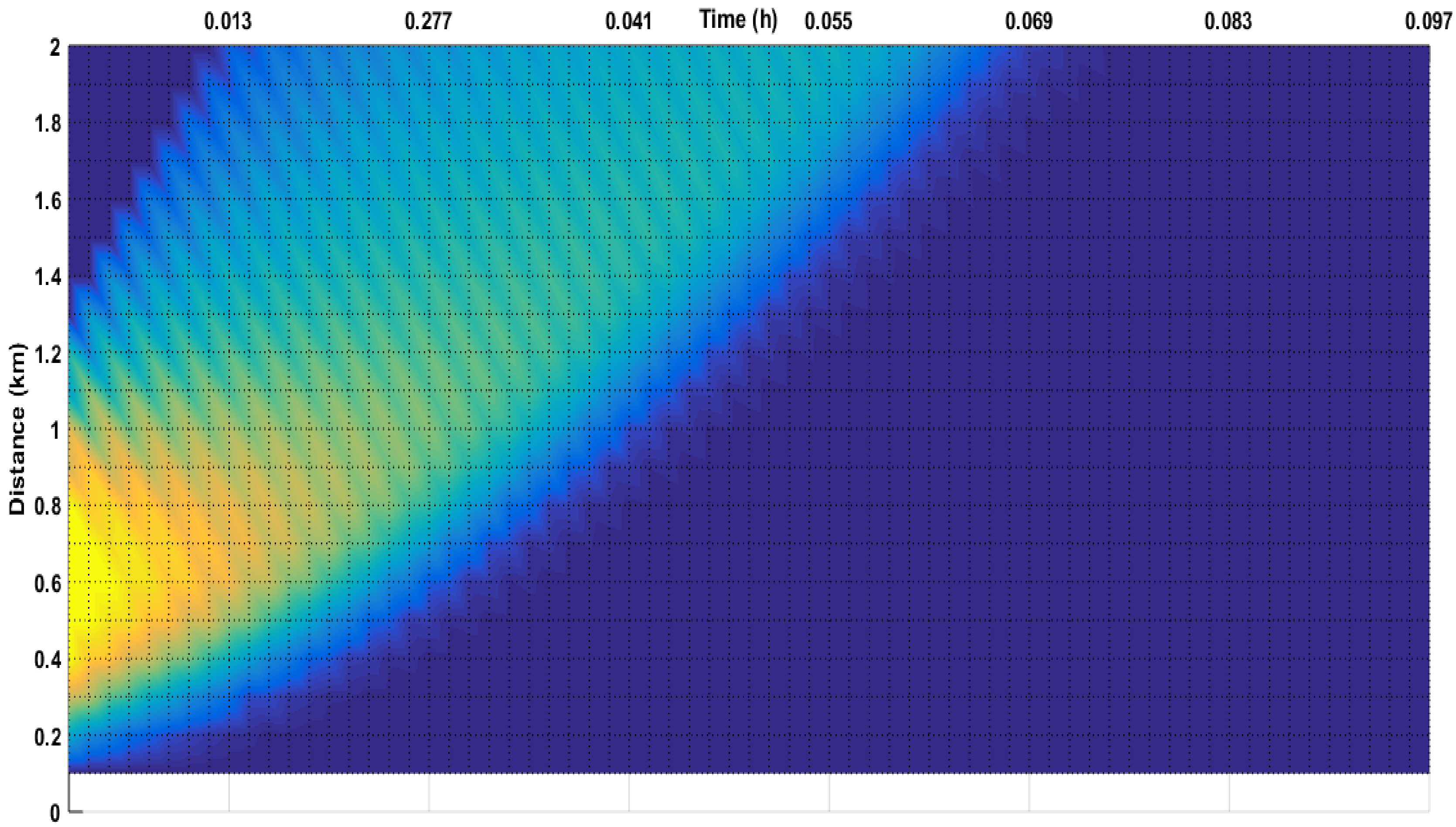

Fig 33: x-t plot showing platoon dispersion of vehicles over 2 km section

Platoon dispersion characteristics of different vehicle classes

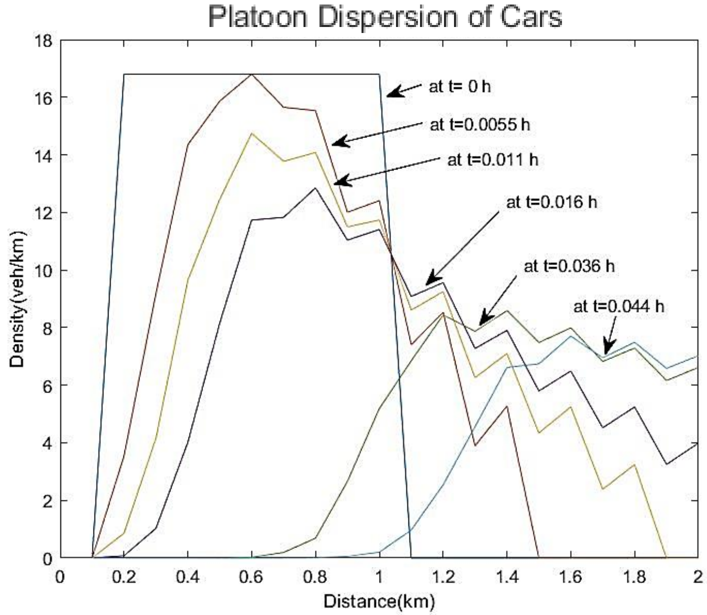

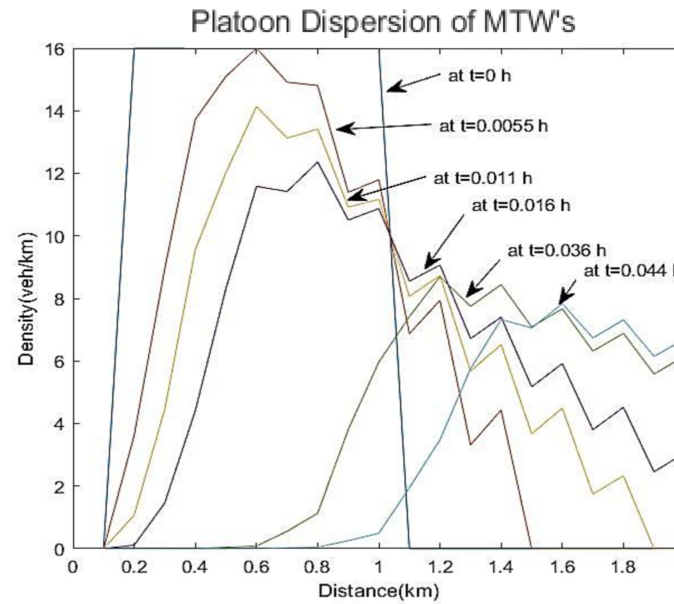

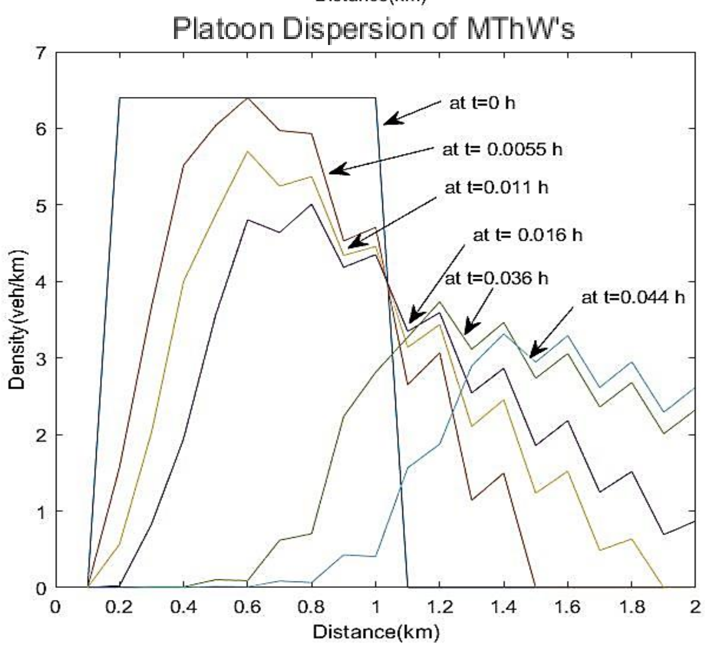

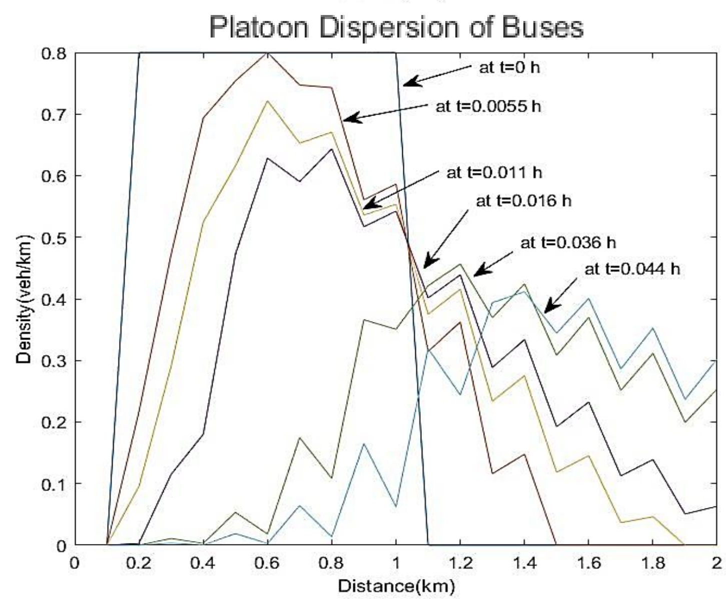

Summary

- Development of NLHT model which considers the following
  - Heterogeneous traffic
  - Two side overtaking
- Calibration
  - GA
  - SA
  - Hybrid
  - Pattern Search
- Sensitivity

References

1. Herrmann, M. and Kerner, B.S., 1998. Local cluster effect in different traffic flow models. *Physica A: Statistical Mechanics and its Applications*, 255(1), pp.163–188. Available at: http://www.sciencedirect.com/science/article/pii/S0378437198001022.
2. Huang, H., Tang, T. and Gao, Z., 2006. Continuum modeling for two-lane traffic flow. *Acta Mechanica Sinica/Lixue Xuebao*, 22(2), pp.132–137.
3. Jiang, R., Wu, Q.-S. and Zhu, Z.-J., 2002. A new continuum model for traffic flow and numerical tests. *Transportation Research Part B: Methodological*, 36(5), pp.405–419. Available at: http://www.sciencedirect.com/science/article/pii/S0191261501000108 [Accessed January 7, 2016].
4. Jin, S., Wang, D., Tao, P. and Li, P., 2010. Non-lane-based full velocity difference car following model. Physica A: Statistical Mechanics and Its Applications, 389(21), pp.4654-4662.
5. Kerner, B.S. and Konhäuser, P., 1993. Cluster effect in initially homogeneous traffic flow. *Physical Review E*, 48(4), pp.R2335–R2338. Available at: https://link.aps.org/doi/10.1103/PhysRevE.48.R2335.
6. Kerner, B.S. and Konhäuser, P., 1994. Structure and parameters of clusters in traffic flow. *Physical Review E*, 50(1), pp.54–83. Available at: https://link.aps.org/doi/10.1103/PhysRevE.50.54.
7. Kerner, B.S., Konhäuser, P. and Schilke, M., 1995. Deterministic spontaneous appearance of traffic jams in slightly inhomogeneous traffic flow. *Physical Review E*, 51(6), pp.6243–6246.
8. Kerner, B.S. and Rehborn, H., 1996a. Experimental features and characteristics of traffic jams. *Physical Review E*, 53(2), pp.R1297–R1300. Available at: https://link.aps.org/doi/10.1103/PhysRevE.53.R1297.
9. Kerner, B.S. and Rehborn, H., 1996b. Experimental properties of complexity in traffic flow. *Physical Review E*, 53(5), pp.R4275–R4278. Available at: https://link.aps.org/doi/10.1103/PhysRevE.53.R4275.

References

10. Payne, H., 1979. FREFLO: A Macroscopic Simulation Model of Freeway Traffic. Transportation Research Record 722, TRB, pp.68–75.
11. Ross, P., 1988. Traffic dynamics. Transportation Research Part B: Methodological, 22(6), pp.421–435.Doi: doi.org/10.1016/0191-2615(88)90023-9
12. Kühne, R.D. and Rödiger, M.B., 1991. Macroscopic simulation model for freeway traffic with jams and stop-start waves. In Proceedings of the 23rd conference on Winter simulation(WSC '91). Washington, DC, USA: IEEE Computer Society:, pp. 762–770. Available at: http://dl.acm.org/citation.cfm?id=304238.304347.
13. Zhang, H.M., 1998. A theory of non equilibrium traffic flow. Transportation Research Part B: Methodological, 32(7),pp.485–498.Doi:doi.org/10.1016/S0191-2615(98)00014-9
14. Berg, P., Mason, A. and Woods, A., 2000. Continuum approach to car-following models. Physical Review E, 61(2), pp.1056–1066. Doi: doi.org/10.1103/PhysRevE.61.1056
15. Gupta, A.K. and Katiyar, V.K., 2006. A new anisotropic continuum model for traffic flow. Physica A: Statistical Mechanics and its Applications, 368(2), pp.551–559. Doi: doi.org/10.1016/j.physa.2005.12.036
16. Zhang, H.M., 2002. A non-equilibrium traffic model devoid of gas-like behavior. Transportation Research Part B: Methodological, 36(3), pp.275–290. Doi: doi.org/10.1016/S0191-2615(00)00050-3

References

17. Tang, C.F., Wu, Q.S., Jiang, R., Wiwatanapataphee, B. and Wu, Y.H., 2007, January. Study of mixed traffic flow in anisotropic continuum model. In Transportation Research Board Annual Meeting, 86th, 2007, Washington, DC, USA.
18. Tang, T.Q., Huang, H.J., Zhao, S.G. and Shang, H.Y., 2009. A new dynamic model for heterogeneous traffic flow. Physics Letters A, 373(29), pp.2461-2466. Doi: dx.doi.org/10.1016/j.physleta.2009.05.006.
19. Nair, R., Mahmassani, H.S. and Miller-Hooks, E., 2011. A porous flow approach to modeling heterogeneous traffic in disordered systems. Transportation Research Part B: Methodological, 45(9), pp.1331–1345. Doi: doi.org/10.1016/j.trb.2011.05.009
20. Gupta, A.K. and Dhiman, I., 2014. Analyses of a continuum traffic flow model for a nonlane-based system. International Journal of Modern Physics C, 25(10), p.1450045. Doi: dx.doi.org/10.1142/S0129183114500454.
21. Mohan, R. and Ramadurai, G., 2017. Heterogeneous traffic flow modelling using second-order macroscopic continuum model. Physics Letters A, 381(3), pp.115-123. Doi: doi.org/10.1016/j.physleta.2016.10.042
22. Li, Y. and Sun, D., 2012. Microscopic car-following model for the traffic flow: the state of the art. Journal of Control Theory and Applications, 10(2), pp.133–143. Doi: dx.doi.org/10.1007/s11768-012-9221-z.
23. Li, Y., Zhang, L., Peeta, S., Pan, H., Zheng, T., Li, Y. and He, X., 2015. Non-lane-discipline-based car-following model considering the effects of two-sided lateral gaps. Nonlinear Dynamics, 80(1-2), pp.227-238. Doi: doi.org/10.1007/s11071-014-1863-6

Thank you.

Questions?

rrkalaga@civil.iitd.ac.in